Reduction of Iron-Bearing Lunar Minerals for the Production of Oxygen

Charles Massieon[1], Andrew Cutler[2] and Farhang Shadman[3]

Department of Chemical Engineering

University of Arizona

Abstract

The kinetics and mechanism of the reduction of simulants of the iron-bearing lunar minerals olivine ($(Fe,Mg)_2SiO_4$), pyroxene ($(Fe,Mg,Ca)SiO_3$), and ilmenite ($FeTiO_3$) are investigated, extending previous work with ilmenite.

Fayalite is reduced by H_2 at 1070 K to 1480 K. A layer of mixed silica glass and iron forms around an unreacted core. Reaction kinetics are influenced by permeation of hydrogen through this layer and a reaction step involving dissociated hydrogen. Reaction mechanisms are independent of Mg content. Augite, hypersthene and hedenbergite are reduced in H_2 at the same temperatures. The products are iron metal and lower iron silicates mixed throughout the mineral. Activation energy rises with calcium content. Ilmenite and fayalite are reduced with carbon deposited on partially reduced minerals *via* the CO disproportionation reaction. Reduction with carbon is rapid, showing the carbothermal reduction of lunar minerals is possible.

---

[1]Graduate Student, Department of Chemical Engineering
[2]Research Assistant Professor, SERC
[3]Professor, Department of Chemical Engineering

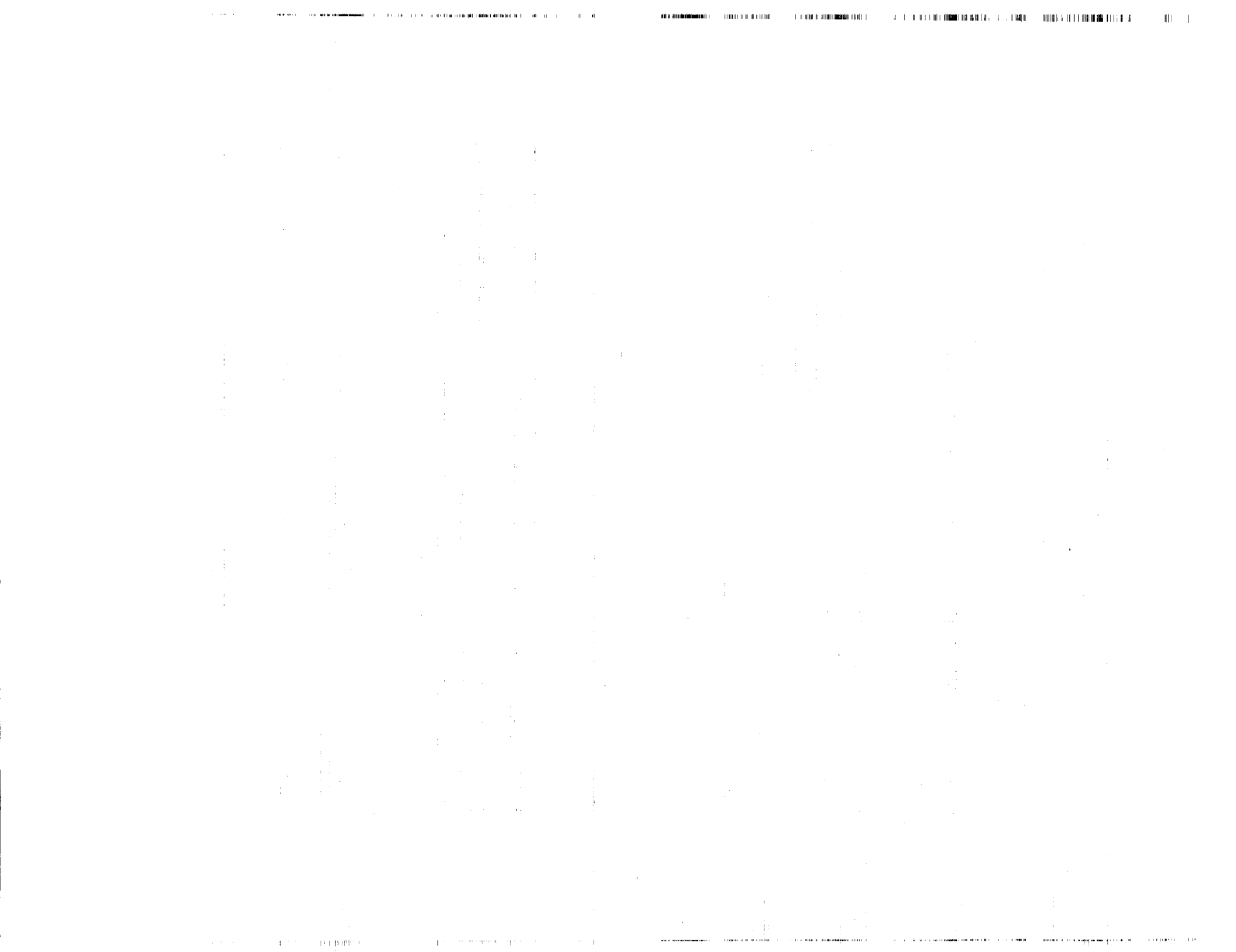

Introduction

Although there is no atmosphere on the Moon, oxygen is available there, since the minerals that make up the Moon's surface are almost entirely oxides (Heiken *et al.*). One of the first activities of a manned lunar base will probably be the production of oxygen for export to Earth orbit, where it will be used as rocket propellant.

The oxygen will be produced by the chemical reduction of oxide minerals. Because the oxygen is tightly bound in the minerals, a fairly strong reducing agent must be used for the reaction to take place, and the selective reduction of the most easily reduced metal ions is likely to be the most economical process. Since strong reducing agents are very rare on the Moon, they will have to be imported from the Earth, and hence very expensive. Thus, any oxygen production process must recycle all but a very small fraction of the reducing agent.

The reducing agents that have received the most attention to date are hydrogen and carbon monoxide, and the mineral which has been most studied is ilmenite ($FeTiO_3$). Typical reactions using these for oxygen production are the reduction of $FeTiO_3$ with hydrogen

$$H_2 + FeTiO_3 \rightarrow H_2O + Fe + TiO_2$$

and the electrolysis of water

$$H_2O \rightarrow H_2 + \frac{1}{2}O_2$$

The hydrogen produced by electrolysis is then recycled to reduce more ilmenite. If carbon monoxide is used instead of hydrogen, carbon dioxide is produced in the reduction step, and it is electrolyzed to form oxygen and carbon monoxide.

Some studies have been done on the design and energy demands of such a project (Cutler, 1986; Cutler and Waldron, 1992; Waldron and Cutler, 1992), but the kinetics of the reduction of lunar minerals must be determined in order to design reactors and make reasonable estimates of design parameters such as energy demands. Because ferrous ions are the most easily reducible of the common metal ions on the Moon, the reduction of iron bearing minerals is of particular interest because it is expected to have the lowest energy cost for the oxygen produced.

Objectives

There are several reasons to consider minerals other than ilmenite and reagents other than H_2 and CO for the production of oxygen on the Moon. One problem with ilmenite is its abundance and distribution on the Moon. Ilmenite is not found in usable concentrations throughout the lunar surface. High ilmenite samples brought back from the Moon have only 10% ilmenite by volume, and many are much lower in the mineral (Heiken *et al*, 1991). Since using lunar soil or rock as feedstock will require heating large amounts of inert solids, beneficiation will probably be necessary and recovering small amounts of ilmenite from the feed will be an expensive process. Further, an early lunar base will not be chosen solely for production of oxygen and may be in an ilmenite poor area, so the ability to handle other minerals may be necessary for the successful operation of an oxygen plant. The iron bearing silicates olivine and pyroxene are more widespread and make up a larger fraction of the rock and soil than ilmenite.

Another reason to study silicates is the mass fraction of oxygen in the mineral available for extraction. The oxygen available in $FeTiO_3$ makes up only 10% of its mass. Available oxygen is 12% of the mass of the pyroxene ferrosilite ($FeSiO_3$), and 16% of the mass of the olivine fayalite (Fe_2SiO_4).

Finally, the equilibrium conversion of the reducing gas is poor. At 1200 K, the equilibrium conversion of H_2 to H_2O by ilmenite is 7.6%, and the equilibrium conversion of CO to CO_2 is 5.9% (Shomate *et al*, 1946). The equilibrium conversion of H_2 by Fe_2SiO_4 is somewhat better (Berliner and Shapovalona, 1966), although for $FeSiO_3$ it is worse (Chase *et al.*, 1985)(Figure 1.1). Because thermodynamic equilibrium is the upper limit on reactor performance, a large fraction of the reducting gas will not be converted in the reduction reactor, so gas reduction processes will be inefficient. Large gas flow rates will be necessary to carry the oxygen from the reactor, which causes problems in gas handling and higher energy demand to heat and cool the gas streams. Fe_2SiO_4 would give some improvement over $FeTiO_3$. Cutler and Waldron (1992) have proposed a countercurrent reactor system, in which pyroxenes are reduced by fresh H_2 coming from the electrolyser, ilmenite is reduced next, and olivines last in order to utilize all three minerals and have conversion as high as possible in the gas stream leaving the reduction reactor. Equilibrium conversion of D_2 is approximately 20% greater than that of H_2 (Cutler, 1991,personal communication), so that its use may improve reactor performance. Reduction with carbon rather than a gas allows complete utilization of the reducing agent and thus lower reactant flow rates. Carbon can be deposited on the iron bearing minerals in a separate deposition reactor. Although

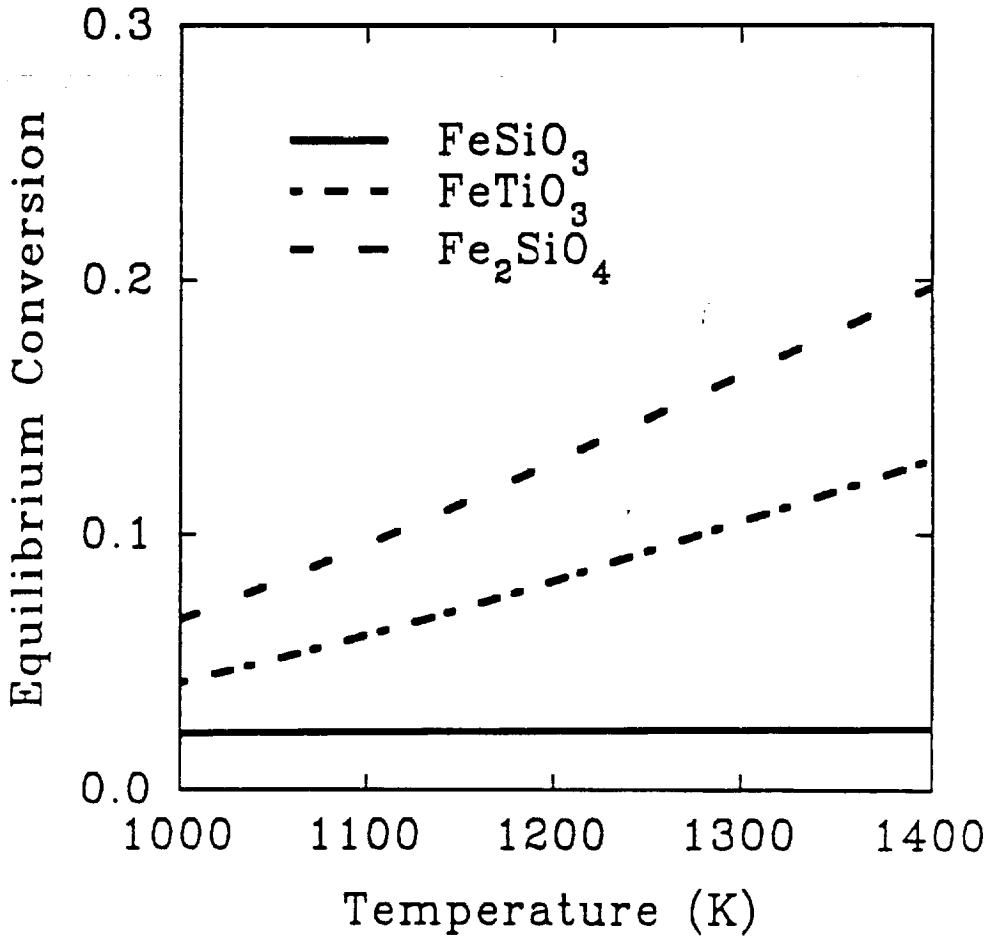

Figure 1.1 Equilibrium Conversion of H_2 by Ilmenite, Fayalite, and Ferrosilite.

this makes the process more complicated, the savings in gas flows may make it worthwhile.

The purpose of this study is to extend the work done on ilmenite to the iron bearing silicates olivine and pyroxene, and to make preliminary investigations on the feasibility of a carbon deposition and reduction process for ilmenite, olivine, and pyroxene. Kinetic parameters such as reaction order, apparent activation energy for these reactions, and the effect of impurities such as magnesium and calcium in the silicates are presented. These parameters should allow future workers in the field of space resources to design and compare oxygen production plants for the Moon.

Ilmenite

The reduction of ilmenite ($FeTiO_3$) with hydrogen and/or carbon monoxide has received the most study to date (Briggs and Sacco, 1990; Zhao, 1991; Zhao and Shadman, 1990 and 1991). The reduction reaction of ilmenite with the reducing agent R can be written as

$$FeTiO_3 + R \rightarrow Fe + TiO_2 + RO$$

During reduction, a product layer of polycrystalline rutile (TiO_2) and iron metal forms. The iron is solid but mobile at reaction temperatures (ca. 1200 K) and migrates to the outside of the reduced grains, leaving the product of iron and rutile separated. Zhao found that the migration of iron plays an important role in the reduction of ilmenite. During the initial period of reduction, the iron has not yet formed nuclei on the outside of the grains, and it accumulates in the pores between rutile crystals, obstructing the diffusion of gases and slowing the reaction. The reaction is first order in both hydrogen and carbon monoxide, and the apparent activation energy is moderate (93 kJ/mol and 75 kJ/mol, respectively).

Olivine

Olivine is a fairly common mineral in the basalts which form the lunar maria, constituting up to 17% of these rocks (Heiken *et al.*). Olivine has the general formula $M^{+2}{}_2SiO_4$, where M^{+2} is any divalent ion close to the size of Fe^{+2}. It forms orthorhombic crystals. The metal ions in naturally occurring olivines are primarily ferrous and magnesium, although manganous ions can be an important impurity. The crystal structure of olivine strongly rejects trivalent ions such as Al^{+3} or Fe^{+3}, so terrestrial olivines make good lunar simulants, unlike terrestrial ilmenite, which contains significant amounts of ferric ion. This work studied the reduction of olivines in the Fe_2SiO_4-Mg_2SiO_4 (fayalite-forsterite) series. A mineral in this series can be regarded as a nearly ideal solid solution of Mg_2SiO_4 and Fe_2SiO_4 (Deer *et al.*). Olivine which is more than 90 mol% Fe_2SiO_4 is called fayalite,

and olivine more than 90 mol% Mg_2SiO_4 is called forsterite. The solution $xFe_2SiO_4 \bullet (1-x)Mg_2SiO_4$ is referred to as Fa_{100x} (or $Fo_{100(1-x)}$ if x is close to zero). The composition of most lunar olivine is about Fa_{20}, but some is close to the end member, Fa_{100}. Since lunar olivines contain some Mg^{+2}, the effect of magnesium on reduction kinetics will be very important to lunar oxygen production.

Gaballah *et al.* (1975) studied the kinetics of the reaction

$$Fe_2SiO_4 + 2H_2 \rightarrow 2Fe + SiO_2 + 2H_2O$$

They found the rate is 1/2 order in H_2 between 1000 K and 1300 K, for p_{H2} between 0.4 atm and 1.0 atm. They found the apparent activation energy to have different values in three temperature ranges: 230 kJ/mol from 1073 K to 1143 K, 263 kJ/mol from 1143 K to 1183 K, and 276 kJ/mol from 1183 K to 1303 K. They attributed these different regions to the phase transitions of quartz to tridymite at 1140 K, and α-Fe to γ-Fe at 1183 K. However, they did not report finding any tridymite in their products, only vitreous silica, quartz and cristobalite. Gaballah *et al.* did not report the amount of crystalline silica found in the products or show powder pattern X-ray diffraction (XRD) plots, and other workers found only traces of quartz or cristobalite (Minowa *et al.* 1968, Watanabe *et al.* 1968, Yanagihara and Kobayashi, 1969). From the activation energy graph published by Gaballah *et al.*, only random scatter about a line corresponding to E=263 kJ/mol can be seen, rather than three different energies. Thus, there is little evidence in their paper to support the claim that the phase transitions of iron and silica are important in the reduction of fayalite. They also found that CO did not react with fayalite to any appreciable extent, which they attributed to the formation of Fe_3C, which increased the volume of solid products and sealed the reaction front from further reaction with CO.

Minowa *et al.* (1968) reduced Fe_2SiO_4 in 1 atm of H_2. Using x-ray diffraction, they found that Fe_2SiO_4 first formed Fe and $Fe_{2-x}SiO_{4-y}$ when reduced, and upon further reduction formed iron metal and amorphous silica. During the initial part of the reduction, the rate followed McKewan's equation, which is the solution of the differential equation

$$\frac{dX}{dt} = k(1-X)^{2/3}$$

with the initial conditions

$$X = 0 \quad at \quad t = 0$$

This equation models a reaction which is controlled by the reactant surface area, which is decreasing as the reaction consumes the solid. The formation of a nonporous layer of products slowed the reduction in the latter part of the reduction, and the data no longer fit McKewan's equation. Minowa *et al.* determined the activation energy for fayalite reduction to be 188 kJ/mol, which was also the activation energy they found for the synthesis of fayalite from quartz and wüstite (FeO). Watanabe *et al.* (1968) reduced fayalite containing some Mg in constant heating rate experiments. They did not extract any kinetic parameters from their data, but observed that Mg greatly slowed the reaction.

The morphology of the solid products has an strong effect on the rate of the reaction. During the reduction of fayalite, the volume of the solids decreases by about 10%. Thus, the products should form a porous polycrystalline layer providing the silica is quartz, tridymite, or cristobalite, but vitreous silica may form a nonporous layer around the fayalite. If the products are porous, the reaction would follow a standard shrinking core model. A nonporous layer may slow the reaction by causing a considerable resistance to mass transfer to and from the reaction front. Since diffusion through a solid is an activated process, the formation of a nonporous layer would not lead to kinetics well represented by a standard shrinking core model. Gaballah *et al.* found quartz and vitreous silica in unspecified amounts in their products at all temperatures, and cristobalite above 1140 K . Their conclusions depend strongly on the formation crystalline silica. Yanagihara and Kobayashi (1968) found only vitreous silica, while Minowa *et al.* (1968) reported that the silica was primarily vitreous with traces of quartz.

Pyroxene

Pyroxene is an extremely abundant and widespread mineral on the moon. Nearly all lunar rocks contain approximately 40% pyroxene by volume (Heiken *et al.*). The chemistry and mineralogy of pyroxene is more complicated than olivine. The general chemical formula of pyroxene is $M^{+2}SiO_3$, where M^{+2} is primarily calcium, magnesium, or ferrous ions. The less rigid crystal structure of pyroxene compared to olivine is reflected in its ability to accommodate up to 1/2 of its metal ions as the relatively large Ca, and also in the ability to substitute trivalent ions for both the divalent metals and the silicon. Pyroxene can crystallize with 2 different crystal structures: orthorhombic for low calcium minerals, and monoclinic for high calcium minerals. The nomenclature of pyroxene is shown in Figure 1.2. In this work, we studied the reduction of three terrestrial pyroxenes with both crystal structures: augite and hedenbergite (both monoclinic) and hypersthene (orthorhombic).

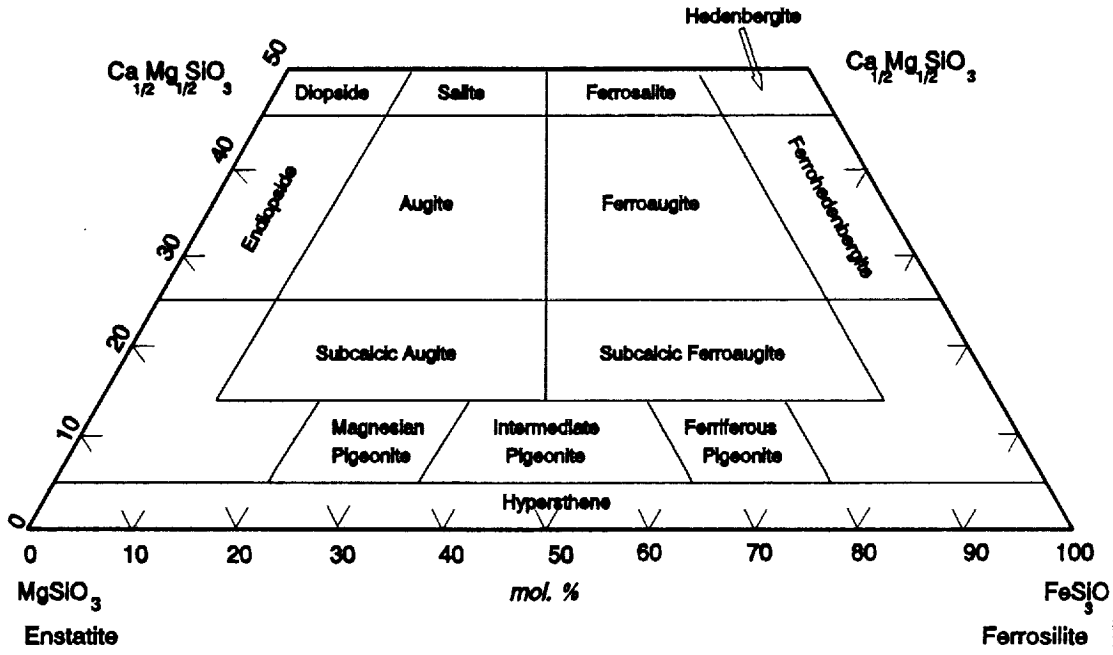

Figure 1.2 Nomenclature of Pyroxenes (after Deer *et al, 1982)*

The reduction of pyroxene has generated less interest than the reduction of olivine or ilmenite. An extensive literature search, including Chemical Abstracts, Engineering Index, and Metallurgical Abstracts, uncovered no literature on the subject, and general texts on pyroxene such as Deer *et al.* do not mention it.

Carbothermal Reduction

Schematics of a carbothermal and CO reduction process for iron bearing minerals are shown in Figure 1.3. For comparison, flows and stream compositions assuming ilmenite feed and equilibrium in the reactors are shown. The gas leaving the carbothermal reduction reactor is assumed to be in equilibrium with carbon rather than ilmenite, since it is in closer contact with carbon just before it leaves the reactor. Although the reactors will not reach 100% efficiency as shown, the reduction of gas flow rates by on order of magnitude and the much higher quality of the gas going to the electrolyser indicate that carbothermal reduction of iron bearing minerals is an appealing alternative to reduction with CO or H_2. It is also possible that carbon may effectively reduce olivine and pyroxene, giving carbothermal processes more flexibility than CO processes.

Thermodynamic equilibrium of the reagents imposes an upper bound on the conversion of a reactor. Good reactor design can approach but never surpass this limit. The low equilibrium conversion of both H_2 and CO by ilmenite (Shomate *et al.*, 1946) causes some severe problems in the reduction process. Although the equilibrium conversion of H_2 by fayalite improves on ilmenite (Figure 1.1), it is still fairly low. As mentioned in the section on fayalite, CO does not react with fayalite to any appreciable extent (Gaballah *et al.*, 1971). Since carbon does not have the equilibrium limitations of the reducing gases, its use makes possible complete utilization of the reducing agent. However, it does introduce some problems of its own. Reduction and electrolysis products are CO and CO_2, and so carbon must be produced from these gases. In order to avoid difficult solid handling and mixing problems, it should be deposited directly on the feed to the reduction reactor. Also, since carbon is scarce on the Moon (Heiken *et al.*, 1991), the loss of any carbon in the spent feed must be avoided. If the gas in contact with Fe product is too high in CO, cementite (Fe_3C) may be produced. If the solids in the reduction reactor are mixed to any extent, some carbon will leave with the spent feed. Removing reducing agents from the solids will require another process step after reduction, and this step will be more difficult with solid carbon than either H_2 or CO.

The reaction this process uses to deposit carbon is the carbon monoxide disproportionation reaction,

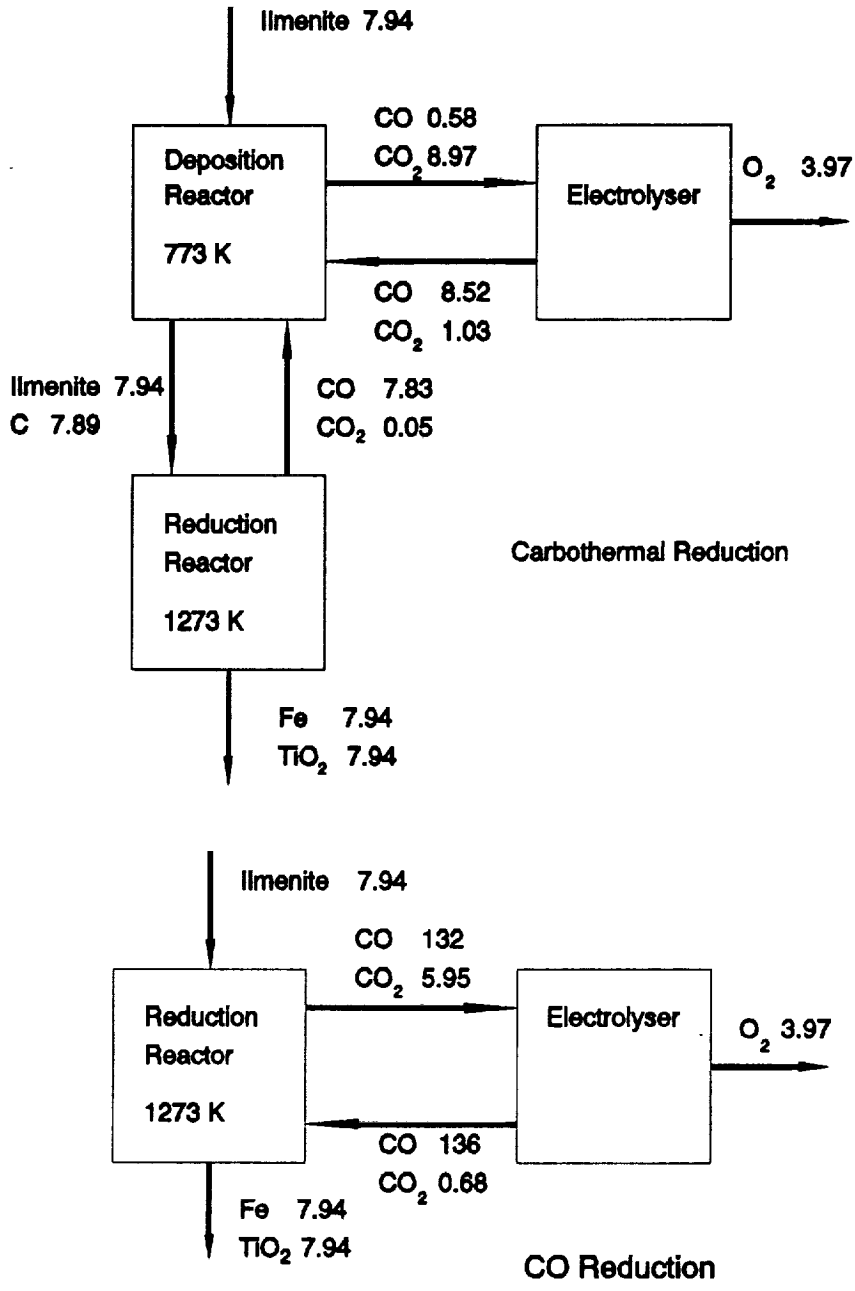

Figure 1.3 Comparison of Carbothermal Reduction and CO Reduction of Ilmenite. Flows in kmol/hr

$$2CO \rightarrow C + CO_2$$

This reaction is thermodynamically favored at 800 K (Wagman *et al.*), but it is slow unless a catalyst is present. Catalysts used for this process will be mixed into and lost with the minerals being reduced, and so must be available in sufficient quantities locally. Iron is a product of the reduction of ilmenite (Zhao, 1991; Zhao and Shadman, 1990 and 1991; Briggs and Sacco, 1991), and is known to be a catalyst for CO disproportionation (Audier *et al.*, 1983; Guinot *et al.*, 1981). Unfortunately, the range of gas compositions in which iron is active is small, and lies outside the range of interest for this process (Audier *et al.*, 1983). The gas compositions of the deposition reactor favor the formation of Fe_3C, which is not catalytically active. The presence of small amounts of H_2 in the gas accelerates CO disproportionation and inhibits the formation of Fe_3C, and H_2 can reactivate Fe_3C (Olsson and Turkdogan, 1974; Turkdogan and Vinters, 1974; Walker *et al.*, 1959). Walker *et al.* found that the amount of H_2 has little effect on the rate between 743 K and 801 K, but has a major effect above 850 K. Above 850 K, they found a gas composition with maximum rate of deposition. Olsson and Turkdogan attributed the effect of small amounts of H_2 to catalytic activity.

Reduced iron-bearing minerals contain iron metal, so some reduced materials could be mixed with fresh feed to supply catalyst for CO disproportionation. A small amount of H_2 could be added to the gas stream to aid carbon deposition. If carbonaceous waste is used to make up reactant losses, it will contain some H_2 from polymers and other sources. Since the equilibrium constant of the CO disproportionation reaction begins to drop rapidly above 800 K, deposition should take place below this temperature. The rate of deposition is sensitive to surface area, and increases as the reaction proceeds. This is due to the fragmentation of iron by growing carbon filaments (Guinot *et al.*, 1981). The iron produced by ilmenite reduction is already in small particles on the outside of the product grains (Zhao and Shadman, 1990; 1991), and is easily accessible as catalyst. The accessibility of the iron product of silicate reduction as a catalyst for carbon deposition needs to be investigated.

Reduction of Olivine With Hydrogen

Experiments

Three olivines of different magnesium content, two fayalites and one forsterite, in the forsterite-fayalite series were used in the reduction experiments. A naturally occurring fayalite with 93% of the metal as Fe and 7% as Mg (Fa_{93}) was purchased from Ward's Natural Science. It is found in rocks from the Forsythe Iron Mine, Hull Township, Quebec, containing Fa_{93}, magnetite, and traces of other minerals. The rocks were crushed to less than 80 μm to give grains of the individual

minerals. Inspection with a microscope confirmed that grains of this size were largely a single mineral. This fayalite is a transparent yellow, and the magnetite and other minerals are very dark or black, which allows easy identification of the fayalite. The magnetite was removed with a small permanent magnet. A Frantz L-1 Isodynamic separator was then used to remove the last traces of the magnetite and also other minerals included in the fayalite matrix. Although experiments were not done to determine specific magnetic susceptibility precisely, the separations performed gave a specific susceptibility between 76×10^{-6} cm^3/g and 100×10^{-6} cm^3/g, which is in the range of values reported for this mineral (Bleil and Petersen, 1982).

The other fayalite, with all metal as Fe (Fa_{100}) was synthesized in our laboratory. A 2:1 molar ratio of wüstite (FeO, 99.9% pure, from CERAC Advanced Specialty Inorganics) and vitreous silica (SiO_2) were mixed. This mixture was then melted in a 1018 steel cup with an oxy-acetylene torch. The oxygen/acetylene ratio of the torch was adjusted to give a slightly reducing flame. The iron of the steel cup ensured that there was no Fe^{+3} in the silicate melt. The melt was then cooled as slowly as possible, so that large crystals of the minerals would form. The product was a mixture of fayalite and either vitreous silica or wüstite, depending on how successfully oxygen had been excluded from the cup during melting. This was then crushed to give grains of the individual minerals, and the fayalite recovered by magnetic separation.

The forsterite was San Carlos peridot purchased from Ward's Natural Science. The Arizona Sonora Desert Museum also donated some sand and rough 1 cm stones of this mineral. The forsterite from Ward's Natural Science is clear light green 1/2 cm tumbled stones. The composition of the mineral from the two sources was the same, and varied from stone to stone between Fa_{14} to Fa_6. Several large stones which showed few inclusions and had a composition of Fa_8 were used for reduction experiments. No mineral separations were necessary, since the stones used had no other minerals in them.

The separated olivines were then analyzed by powder pattern X-ray diffraction (XRD) (Figures 2.1 and 2.2) and scanning electron microscopy with energy dispersive X-ray spectroscopy (SEM/EDS) to identify the minerals and determine their composition. The bulk composition was also determined using atomic absorption spectroscopy.

The olivine was ground, washed in acetone to remove fines, and sieved, and the fraction between 38μm and 45μm was pressed into disks 8mm in diameter and 0.6 mm thick. These were cut into

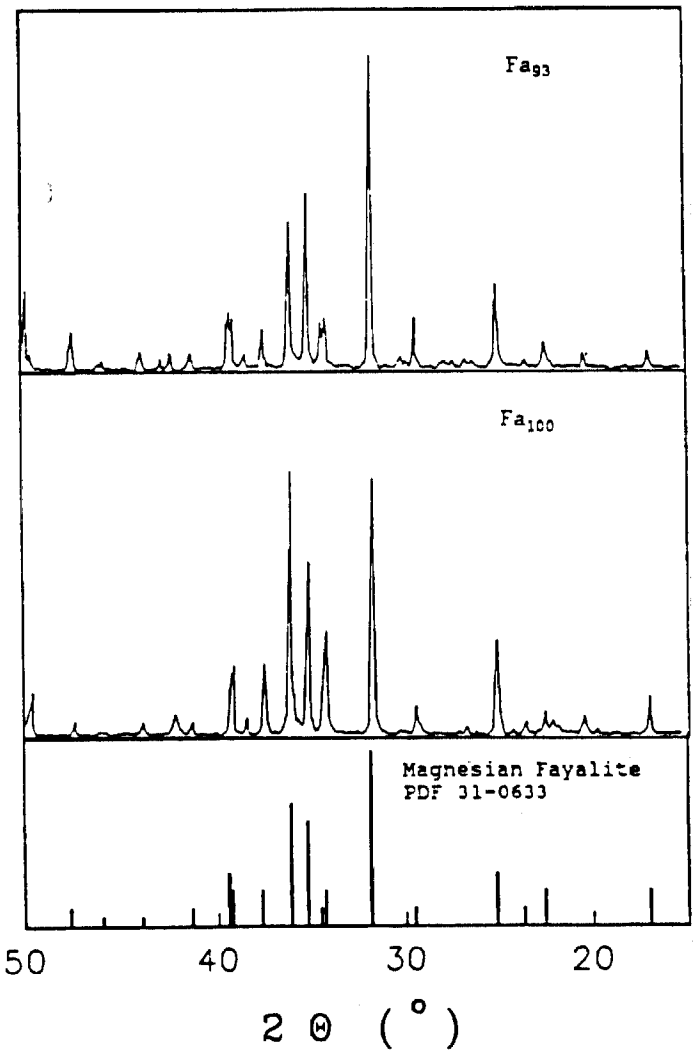

Figure 2.1 Powder Pattern X-ray Diffraction of Fayalite

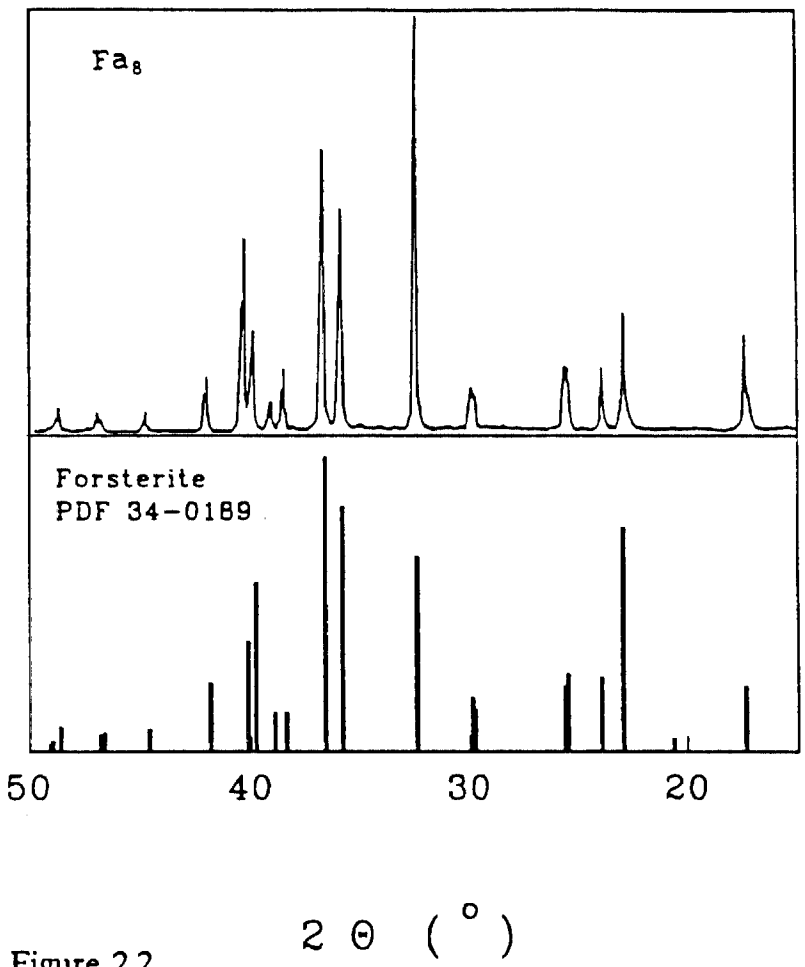

Figure 2.2 Powder Pattern X-ray Diffraction of Forsterite

rectangular flakes, approximately 5mm × 6mm. The dies used by Yi Zhao (Zhao, 1991) for the preparation of ilmenite pellets were made of 316 stainless steel, and were too soft for use with silicates. The pistons bent and galled in the die body, causing irreparable damage to the die. This problem was solved by making the die bodies of hardened 416 stainless steel, and the pistons of air hardened A2 tool steel. Zhao (1991) had shown that these pellets did not cause any significant mass transfer resistance for ilmenite experiments done in our lab, so they should not cause any for reactions with silicates, which are slower than those with ilmenite.

A schematic of the reactor system used in our experiments is shown in Figure 2.3. The system consisted of a gas mixing section, a Cahn 1000 electronic microbalance, a quartz glass reactor, a moveable furnace with controller, and a nondispersive infrared CO/CO_2 analyzer and gas chromatograph downstream of the reactor. All experiments were done at ambient pressure, 0.93 atm. Reaction progress was continuously monitored with the electronic balance and the output recorded with a strip chart recorder and a computer data acquisition system. The gas chromatograph was used to set up the gas before the reaction, but could not be used during an experiment because it caused flow and pressure variations in the reactor. The mineral sample was placed in a Pt wire basket suspended from the balance. The reactor system was then closed and purged with 99.999% pure N_2 for at least 3 hours to remove oxygen. Then the flow of reacting gas was started. The flow was 400 cm^3/min at 0.93 atm and 295 K in all experiments. Zhao (1991) showed that this flow eliminated all interphase mass transfer resistance in the same reactor system with faster ilmenite reactions, so it sould also do so in these experiments. When the system stabilized, the reaction was started by quickly raising the furnace. The temperature in the reactor, measured with a type K thermocouple, stabilized at its final value in 2 or 3 minutes. The furnace was lowered at the end of the experiment, which caused the reactor temperature to decrease very rapidly and quench the reaction. Gas flow past the sample caused the weight reading to increase due to drag. The drag was measured as the difference between the weight just before lowering the furnace and after all gas flow had stopped. The drag was subtracted from the weight readings taken during the experiment to give actual weights. Because the drag depends on reactor temperature, weight readings could not be used until the temperature stabilized at the start of an experiment. Experiments were performed to determine the amount of adsorbed volatiles. In these experiments, the reactor was brought to reaction temperature in N_2, and then the H_2 flow was started. There was some loss of volatiles, and this loss was estimated for each run and subtracted from the initial mass.

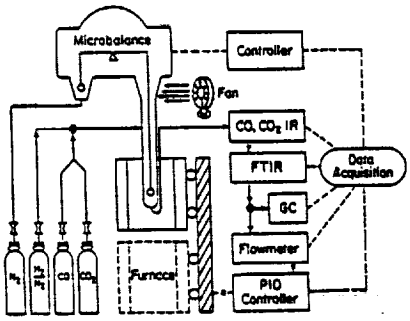

Figure 2.3 Schematic of the Reactor System
IR: Non-dispersive infrared analyzer; GC: gas chromatograph

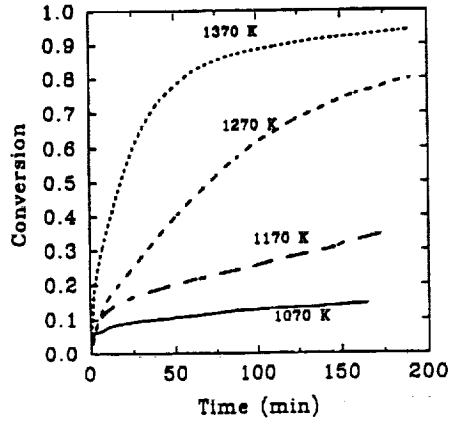

Figure 2.4 Reduction of Fa_{93} in 0.14 atm H_2

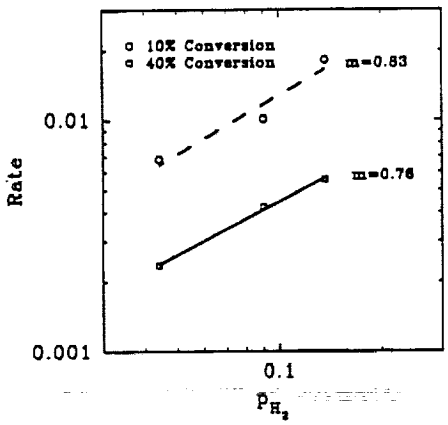

Figure 2.5 Effect of Hydrogen Partial Pressure on the Reduction of Fa_{93}

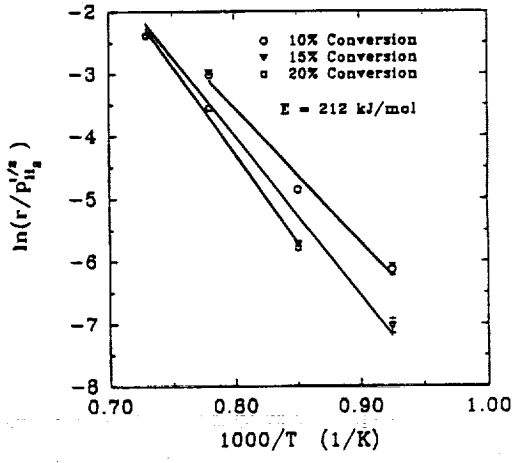

Figure 2.6 Apparent Activation Energy of the Reduction of Fayalite with H_2

Samples of the solid reaction products were mounted in epoxy and polished at Buehler Southwest Research Laboratory. This reveals the particle cross sections for SEM/EDS analysis. SEM micrographs were made with backscattered electrons. Backscattered electron signal strength is primarily a function of average atomic number, so regions with high average atomic number such as high iron phases are brighter than low average atomic number regions. Other samples were ground for XRD. Single crystal silicon slides were used for XRD in order to eliminate any interfering signal from the slide, and so that glass, which produces a low, broad, and noisy signal at low angles, could be positively identified as part of the sample. The combination of SEM/EDS analysis and powder X-ray pattern diffraction allowed conclusive identification of the products.

Results

The naturally occurring fayalite, Fa_{93}, was reduced with mixtures of 0.047 to 0.14 atm H_2 in N_2 at a total pressure of 0.93 atm and at temperatures from 1070 K to 1370 K. Figure 2.4 shows the temporal profile for these reactions in 0.14 atm H_2 at 1070, 1170, 1270, and 1370 K. Conversion in the plot is the fraction of the iron in the mineral that has been reduced to metallic iron. These curves show that the reduction proceeded rapidly until conversion was about 15%, and then slowed considerably. The effects of H_2 concentration are shown in Figure 2.5. The reduction of Fa_{93} is 0.8 order in H_2. This is somewhat higher than the findings of Gaballah *et al* for Fa_{100} at $0.4 \text{ atm} \leq P_{H2} \leq 1 \text{ atm}$. The activation energy didn't change in the course of the reaction. The apparent activation energy is 212 ± 5 kJ/mol (Figure 2.6), much lower than the values reported by Gaballah, but slightly higher than that of Minowa.

Figure 2.7 is an SEM micrograph of a typical grain of partially reduced Fa_{93}. The medium grey core of the grain is fayalite of the same composition as the starting material. The core is surrounded by a layer of very finely mixed iron and silica. The two small grey areas at the lower right of the product layer have a metal to silicon ratio close to 1, characteristic of pyroxene rather than olivine. Mg and Mn in these two areas are slightly enriched relative to Fe as compared to the starting material. The SEM micrograph of nearly fully converted Fa_{93} (Figure 2.8) shows almost all of the fayalite has been converted to a mixture of silica and iron. The two medium grey areas near the top of the grain are olivine, considerably enriched in Mg and Mn from the starting material. The lighter regions in the relatively dark silica phase seem to have some Mg, although they are too small for accurate EDS analysis.

Powder pattern XRD of partially and fully reduced Fa_{93} is shown in Figure 2.9. The only crystalline

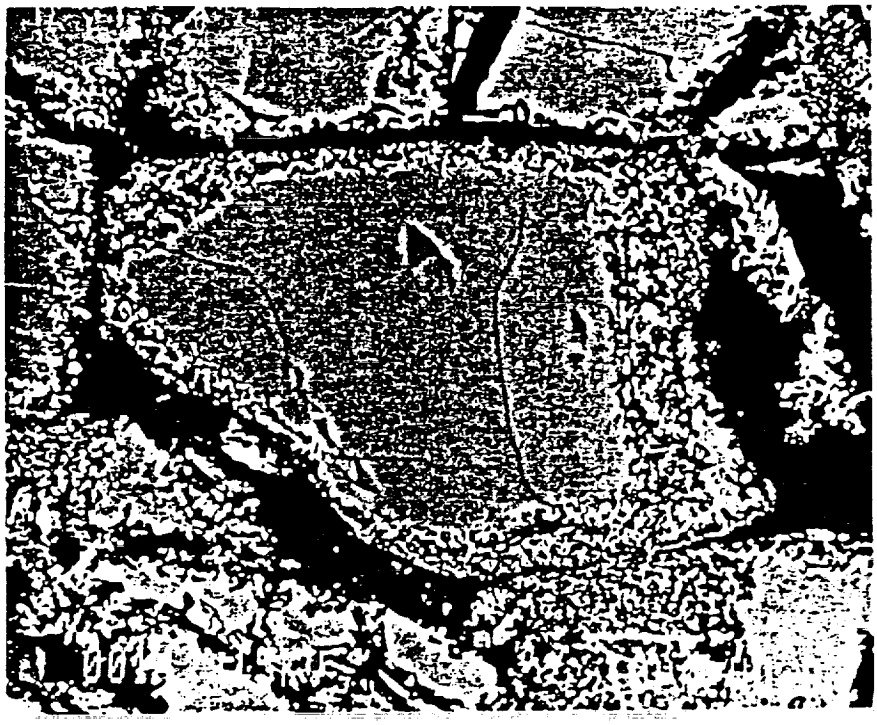

Figure 2.7 SEM Micrograph of a Cross Section of Partially Reduced Fa_{93}

Figure 2.8 SEM Micrograph of a Cross Section of Completely Reduced Fa_{93}

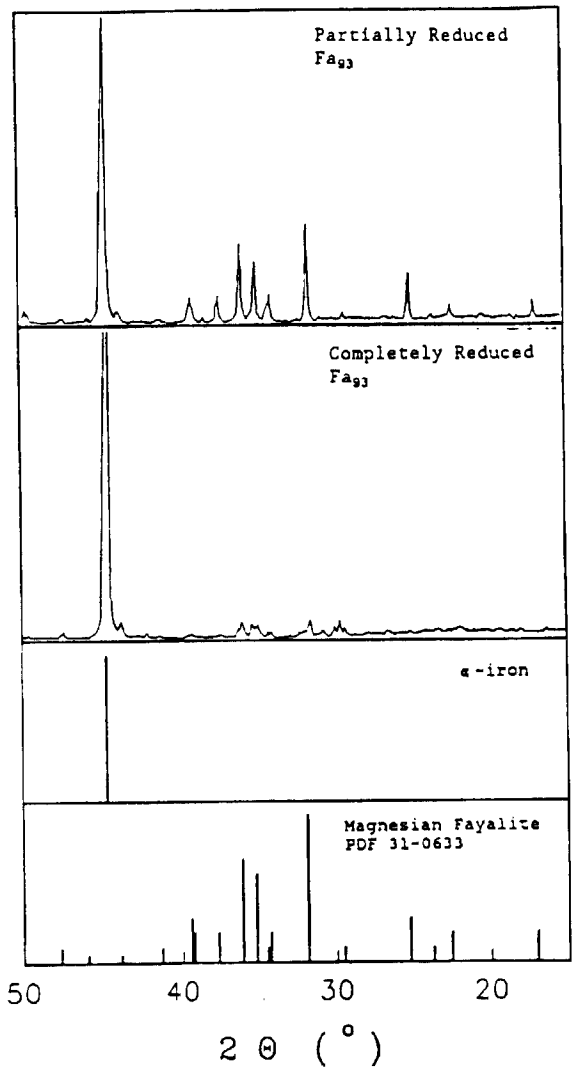

Figure 2.9 Powder Pattern X-ray Diffraction of Reduced Fa_{93}

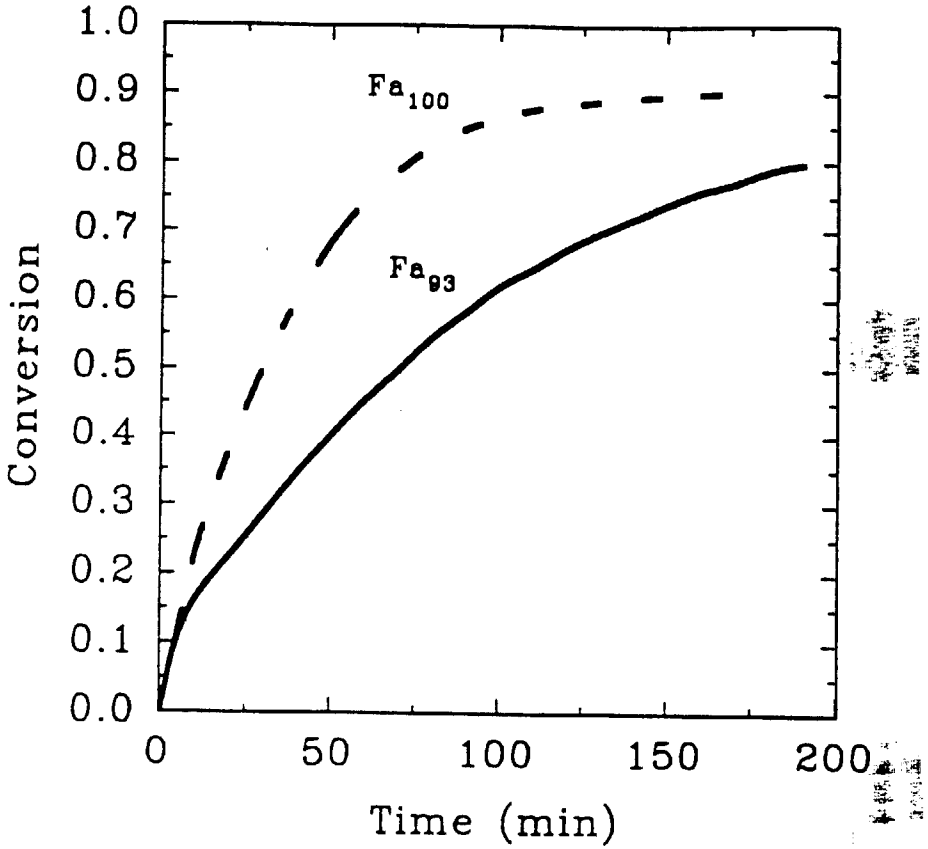

Figure 2.10 Effect of Magnesium on the Reduction of Fayalite with H_2

phases appearing are fayalite and iron. The noise at low 2θ indicates a glassy phase. The XRD pattern of fully reduced Fa_{93} shows mostly iron with a small amount of olivine remaining. The olivine pattern is shifted slightly from Fa_{93}, indicative of a more Mn rich mineral. Only evidence of vitreous silica, and no quartz, tridymite, or cristobalite is seen in the XRD patterns of fully and partially reduced Fa_{93}.

To study the effects of Mg on the reduction of fayalite, Fa_{100} was prepared in our laboratory. The reduction of fayalite is slowed greatly by small amounts of magnesium (Figure 2.10), and the temperature at which reduction occurs at an appreciable rate is increased. The apparent activation energy for reduction of Fa_{100} is 200 ± 8 kJ/mol (Figure 2.11), again much closer to Minowa's value than Gaballah's. Figure 2.12 is a cross section near the end of a grain of partially reduced Fa_{100}. It has a layer of finely mixed iron and silica surrounding the core. Grains sectioned through the middle (for instance, the small grains on the far right of the micrograph) have a uniform core of fayalite, but the core of this grain has a mottled appearance, and EDS gives an iron to silica ratio close to 1, as for a pyroxene, but which varies with Fe slightly higher in the brighter areas. No pyroxene can be detected in the XRD pattern of this material (Figure 2.13), and none was present in the starting material. We believe that this is a section through the reaction front, and that this is evidence that the iron is reduced in the fayalite matrix, and then migrates out towards the layer of mixed Fe and silica, leaving a thin zone deficient in iron and oxygen compared to fayalite, but which has not yet formed silica and iron. Figure 2.14 shows a grain of nearly completely converted Fa_{100}. This is the more typical situation of a fayalite core surrounded by mixed iron and silica. As before, the only crystalline phases indicated by XRD are Fe and fayalite.

The reduction experiments with Fa_8 did not yield reproducible results. The combination of extremely small mass changes and long experiment times was partly the reason. Figure 2.15 shows the conversion in a typical run at 1387 K in 0.14 atm H_2. The period of slow reduction at the start occurred in all runs, but was of highly variable length. Experiments done at lower temperatures did not produce any measurable reaction. Figure 2.16 is an SEM micrograph of a cross section of partially reduced Fa_8. The bright spots are Fe, the light streaks are regions of high Fe, and the grey regions are Fa_8. No silica phases could be found, and XRD revealed only olivine, since the amount of Fe produced was below detectability limits of the diffractometer.

Discussion

Although the presence of small amounts of magnesium greatly affects the reduction rates of fayalite,

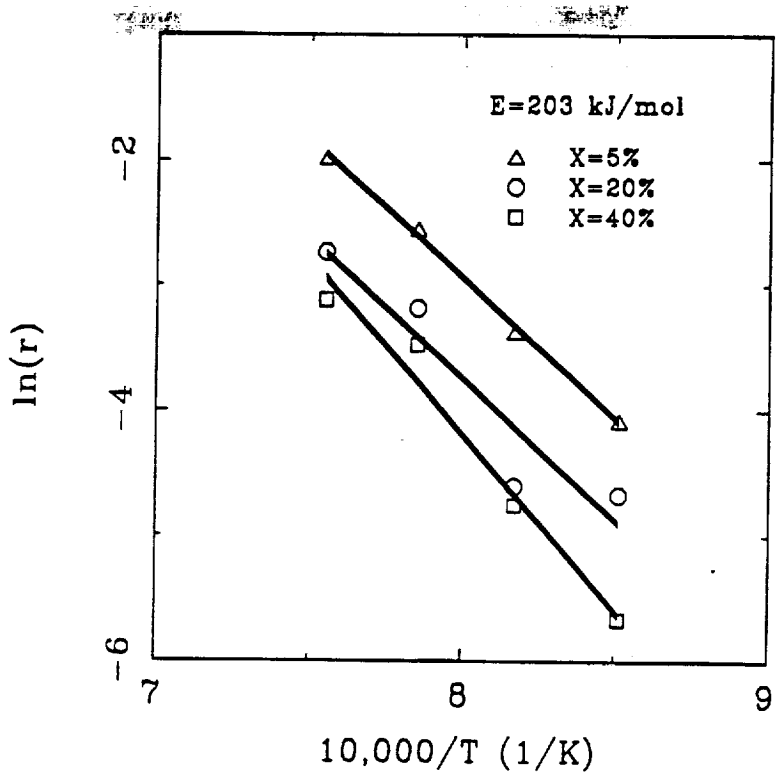

Figure 2.11 Apparent Activation Energy of the Reduction of Fa_{100} with H_2

Figure 2.12 SEM Micrograph of a Cross Section of the Reaction Front in Partially Reduced Fa_{100}

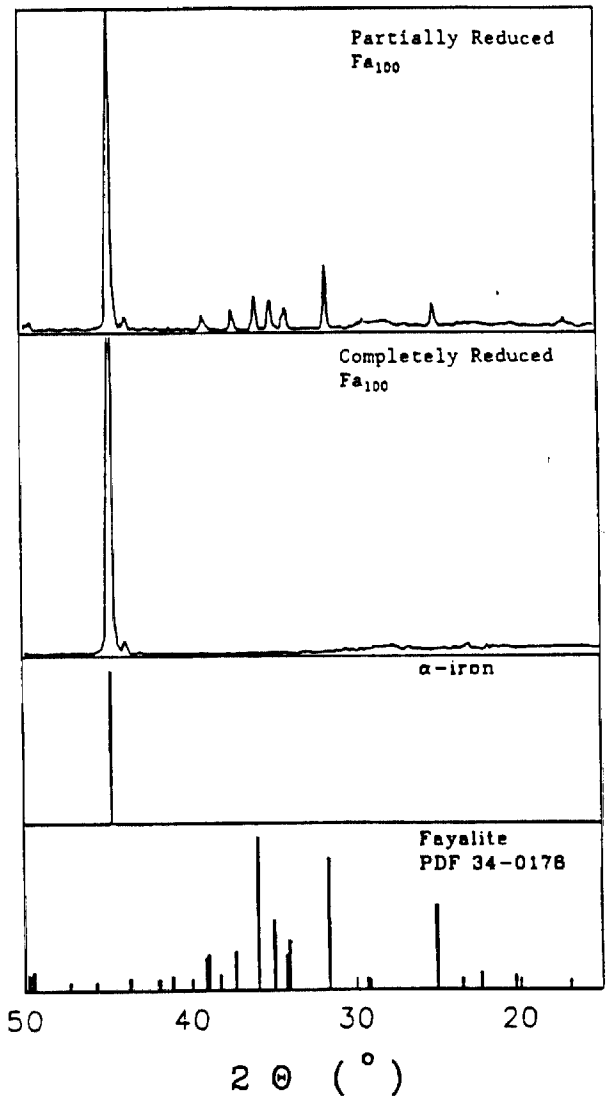

Figure 2.13 Powder Pattern X-ray Diffraction of Reduced Fa_{100}

Figure 2.14 SEM Micrograph of a Cross Section of Completely Reduced Fa_{100}

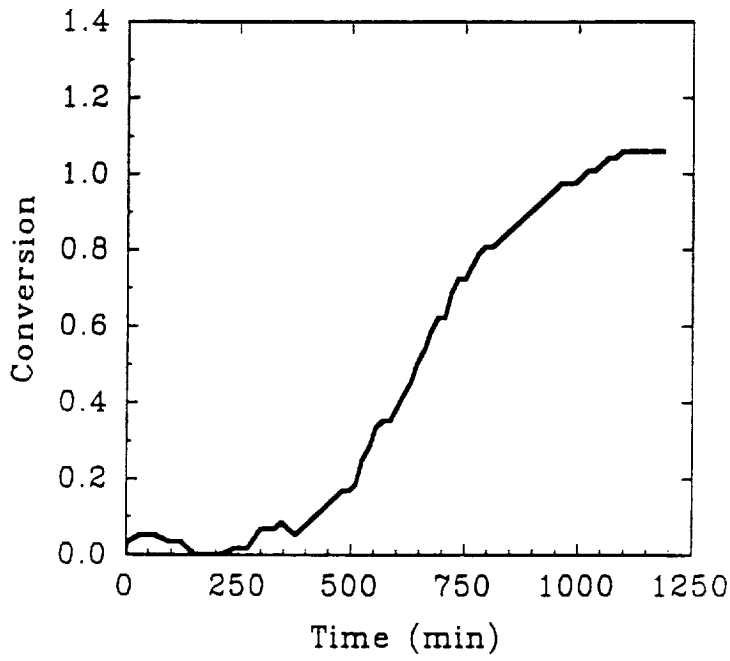

Figure 2.15 Reduction of Fa_6 in 0.14 atm H_2 at 1387 K

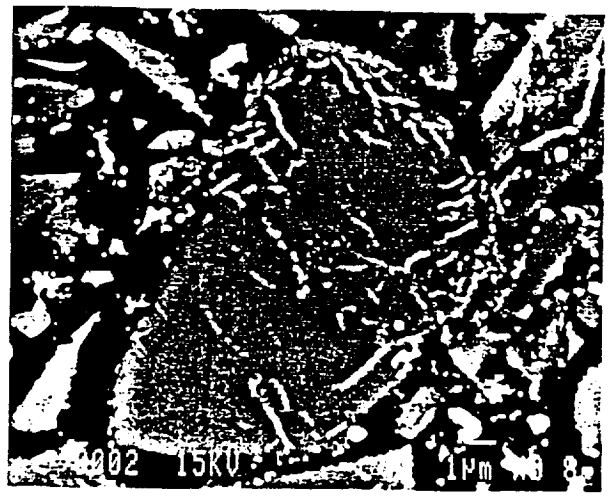

Figure 2.16 SEM Micrograph of a Cross Section of Partially Reduced Fa_3

it does not seem to change the mechanism of the reaction. As shown in Figure 2.10, the effect of magnesium on reaction rates is too great to be acting simply as a diluent of the iron. The rate is 0.8 order in p_{H2} between 0.047 and 0.14 atm, somewhat greater than the 1/2 power dependence determined by Gaballah *et al.* at hydrogen partial pressures between 0.4 atm and 1.0 atm for Fa_{100}. Magnesium does not have an affect on the apparent activation energy in this range of compositions, either. The activation energies we determined, 212 ± 5 kJ/mol for Fa_{93} and 203 ± 8 kJ/mol for Fa_{100}, are much closer to the value determined by Minowa *et al.* (188 kJ/mol) than those of Gaballah *et al.* (263 kJ/mol). The activation energy is close to that found by Minowa for the formation of Fe_2SiO_4 from quartz and FeO. In materials where diffusion through the pores dominates reaction kinetics, the apparent activation energy approaches 1/2 the intrinsic activation energy as the reaction approaches completion. In the reduction of fayalite, activation energy does not vary with conversion, so the diffusion of gases through pores in the product layer is not important. The distribution of iron throughout the product also suggests that the silica formed is not porous. Iron, although solid, is mobile at these temperatures and tends to agglomerate. In the case of ilmenite, where the solid product is polycrystalline rutile and iron, the iron diffuses along the surface of the pores in the rutile and forms large particles on the outside of the product layer (Zhao and Shadman,1991). Formation of a nonporous silica layer would also explain the extremely slow rate of reduction of fayalite by CO observed by Gaballah *et al.*, since silica glass is virtually impermeable to CO and CO_2.

SEM and XRD analysis shows that metallic iron mixed with amorphous silica forms a nonporous layer around a core of unreduced fayalite. Magnesium and manganese, less reducible than iron, migrate to stay in the fayalite. During the course of the reaction, the concentration of iron in the fayalite being reduced gradually decreases. No gradients of Mg were observed in the core with SEM/EDS, although the diffusivity of Mg in fayalite is of order of magnitude 10^{-12} cm^2/sec (Deer *et al.*), and the characteristic time for diffusion across a grain is 4000 hr. Pyroxenes, such as $FeSiO_3$, do not form as an intermediate product, and the SiO_2 does not crystallize. Pyroxenes which could be produced in the compositions studied here are not thermodynamically stable (Bowen and Shairer, 1935). Phase transitions between SiO_2 polymorphs requiring rearrangement of the Si-O lattice are slow, and the formation of pyroxene or crystalline SiO_2 (quartz, trydimite, or cristobalite) would require extensive reordering of the Si-O lattice in fayalite (see, for example, Deer *et al.*, 1982). Since pyroxene is not thermodynamically stable, and rearrangement of oxygen-silicon lattices are slow, pyroxene is not formed as an intermediate, and the silica formed is amorphous. During reduction, the x-ray diffraction pattern of fayalite gradually disappears except for a peak

corresponding to 0.207 nm (at $2\theta = 43.8^{\circ}$) (Figures 2.9 and 2.13). Minowa *et al.* reported a similar peak at 0.222 nm. This distance is approximately the average distance between the M^{+2} and oxygen ion in fayalite (0.2072 nm to 0.2291 nm) (Birle *et al.*, 1968), and may indicate the preservation of some of the fayalite crystal structure in the silica. Evidence of the $Fe_{2-x}SiO_{4-y}$ intermediate proposed by Minowa is shown in Figure 2.12, an SEM micrograph cross section of the end of a grain of partially reduced Fa_{100}. The section goes through the reaction zone. In this area, the composition is variable, with an Fe/Si ratio of around 1. This ratio is characteristic of a pyroxene, but no pyroxene is detected in such samples by XRD. The brighter regions in the mottled area are higher in Fe, and appear to be regions where Fe is beginning to agglomerate. The brighter, uniform cores of the small grains on the right of the micrograph are fayalite. Since the iron does not form larger agglomerations near the outside of the grains where it has had longer to migrate than near the reaction zone, it appears that the formation of vitreous silica immobilizes it. Thus, during reduction the grains of fayalite are divided into three regions: an inner core of unreacted fayalite, a very thin layer of FeO deficient intermediate which retains some of the fayalite crystal structure, and an outer layer of mixed iron metal and amorphous silica. The iron is mobile in the intermediate product, and forms small agglomerations, but is immobilized when the fayalite structure is converted to amorphous silica. Hydrogen must cross the layer of silica glass to reach the reaction front, and the water produced must cross it to leave. The permeability of hydrogen in silica glass is first order in H_2 with an activation energy of 37.2 kJ/mol (Lee *et al.*, 1962). The permeability does not depend on the OH or metal impurity of the glass and is probably due to diffusion of H_2 molecules through interstitial sites in the silica (Lee, 1963). Since the reduction of fayalite is lower order in H_2 and the apparent activation energy is 212 kJ/mol, permeability of silica to H_2 does not completely control the reaction kinetics. A calculation based on the conditions shown in Figure 2.7 shows that hydrogen transport through the silica does influence the kinetics of fayalite reduction. The permeability of hydrogen in silica at 1270 K is 2.5×10^{-12} mol H_2/cm-atm-s (Lee *et al.*, 1962). If one assumes that the grains are cubes 40 μm on a side with a 1.5 μm layer of silica, the reaction rate corresponding to maximum H_2 transport is 5.4×10^{-3} min^{-1}. The observed rate for this reaction is 4.2×10^{-3} min^{-1}. This indicates that permeation of H_2 through silica is important in the reaction kinetics, although H_2 order and activation energy indicates that it is not controlling. Chemical solubility of hydrogen as OH groups on the Si-O lattice predominates over physical solubility as H_2 molecules in vitreous silica at temperatures above 800 K (Shackleford and Masaryk, 1976), and the solubility is proportional to $p_{H2}^{1/2}$ (Bell *et al.*, 1962). The hydroxyl radicals are much more reactive than H_2 molecules, and are possibly an intermediate species in the reaction. Lee (1963) found that the chemical solubility of hydrogen is dependent on the formation and thermal history of the silica,

so estimates of the OH content of the silica formed during the reaction cannot be made from available data. Shackleford and Masaryk determined the binding energy of dissociated H species in silica glass to be about 260 kJ/mol, somewhat higher than the apparent activation energy of reduction. Partial control of the rate by the less activated permeation of H_2 in silica would reduce the apparent activation energy from this value, and give a reaction order in H_2 between those of permeation and dissociation of hydrogen.

From this evidence, the reaction kinetics of fayalite with hydrogen are partly determined by the permeation of H_2 through vitreous silica which forms a layer around the partially reacted fayalite, and partly by a step involving chemical reaction of hydrogen with the fayalite. The chemical reaction may be the dissociation of H_2 into hydroxyl groups on the Si-O lattice. The substitution of magnesium for ferrous ions in fayalite slows reaction with H_2 more than expected if it simply acted as a diluent. Magnesium and manganous ions diffuse to stay primarily in the fayalite. Although we could not detect it, magnesium may be concentrated near the reaction zone since it diffuses through fayalite very slowly. This would amplify the effect of magnesium on reaction rates. Magnesium also stabilizes the fayalite structure, as shown by its effect on melting temperature (Bowen and Shairer, 1935), which could contribute to its slowing of the reaction. The stabilization of fayalite by magnesium would also explain the results of the experiments with Fa_8, which reacted extremely slowly, and did not form a silica phase.

Reduction of Pyroxene With Hydrogen

Experiments

Reduction experiments were performed on three different pyroxenes. Two of these, augite (a clinopyroxene) and hypersthene (an orthopyroxene) are common in samples returned from the Moon (Heiken *et al.* 1991). The third, hedenbergite (a clinopyroxene), is less common, but provides useful results on the effect of iron concentration on reaction kinetics and mechanism. All three minerals were purchased from Ward's Natural Science. The augite is in approximately 1/2 cm crystals from Cernosin in the former U.S.S.R. SEM and XRD analysis showed that the crystals have few inclusions, and were not compositionally zoned. The chemical composition of the augite is $Fe_{0.13}Mg_{0.44}Ca_{0.43}SiO_3$. The hypersthene is large rocks from St.-Ludger-de-Milot, Quebec. It, too, was reasonably uniform. Its chemical composition is $Fe_{0.19}Mg_{0.79}Ca_{0.02}SiO_3$. No separations were performed on these two minerals. The hedenbergite is a minor constituent of the fayalite/magnetite rocks from the Forsythe Iron Mine, Hull Township, Quebec. It was recovered during the magnetic

separations of this rock, and contains some ferrosilite. The mass susceptibilities of hedenbergite and ferrosilite are close, and these two minerals could not be separated. The chemical composition of the hedenbergite is $Fe_{0.43}Mg_{0.10}Ca_{0.47}SiO_3$ and the ferrosilite is $Fe_{0.93}Mg_{0.07}SiO_3$.

The experimental procedure for pyroxene is the same as that for olivine. Samples of the reaction products were prepared for SEM/EDS and XRD as before.

Results

The hypersthene was reduced in 0.14 atm H_2 at 1190 K, 1280 K, and 1390 K (Figure 3.1). Mass changes during these experiments were small, and took place over long time periods, but the results were repeatable, unlike those for Fa_8. The majority of the mass loss took place in the first few minutes of the experiment, when the reactor system had not yet stabilized. After the initial mass loss, the rate of reduction was slow and close to constant. To obtain an estimate of the apparent activation energy, we fit a line to the constant rate portion of the reduction curve, and used the slope as the rate of reaction. The apparent activation energy is 72 kJ/mol (Figure 3.2). An SEM micrograph of partially reduced hypersthene is shown in Figure 3.3. The brightest areas are iron, the light grey is $MgTiO_3$, and the dark grey is hypersthene. The band of iron and $MgTiO_3$ is probably a reduced ilmenite inclusion. A few small grains have small specks of iron in a matrix of hypersthene and a darker material. The dark regions are too small for EDS analysis, but may be silica or a low iron pyroxene.

The augite was reduced in 0.14 atm H_2 at 1090 K, 1180 K, 1280 K and 1380 K (Figure 3.4). The iron content of the augite is less than that of the hypersthene, and so mass loss during the experiments was smaller. The augite showed the same drop in mass during the first few minutes of an experiment as hypersthene. After that, the rate was fairly steady, although less so than for hypersthene. The apparent activation energy of the reduction of augite with H_2 was estimated in the same way as that of hypersthene. The estimated activation energy is 150 kJ/mol (Figure 3.5). Figure 3.6 is an SEM micrograph of a cross section of partially reduced augite. The only phase large enough for EDS analysis is augite. The extremely bright specks are probably iron. A small grain of augite with some bands of darker material containing iron specks can be seen in the lower center of the photo.

Hedenbergite was reduced in 0.14 atm H_2 at 1170 K, 1270 K, and 1370 K (Figure 3.7). It, like the other pyroxenes, showed a rapid rate in the initial period of the reaction, followed by a slower,

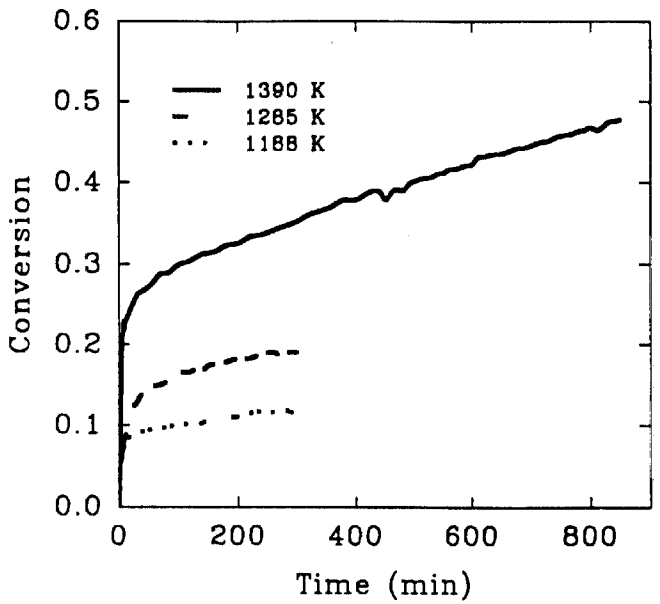

Figure 3.1 Reduction of Hypersthene in 0.14 atm H_2

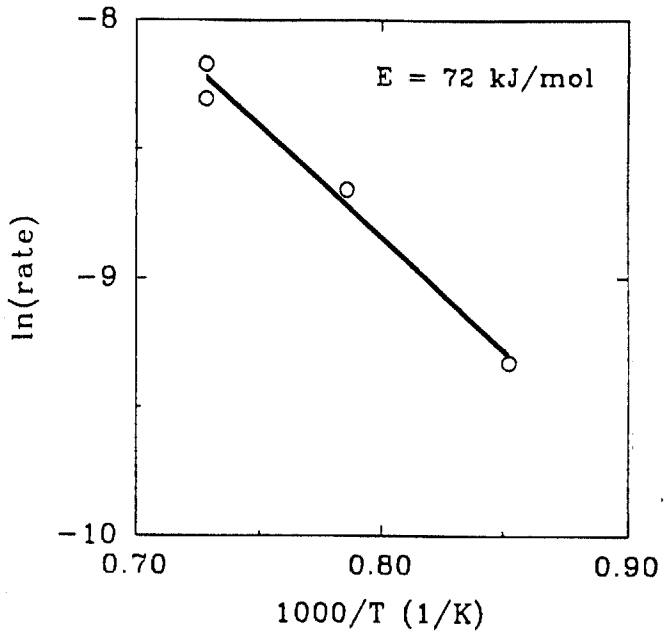

Figure 3.2 Apparent Activation of the Reduction of Hypersthene with H_2

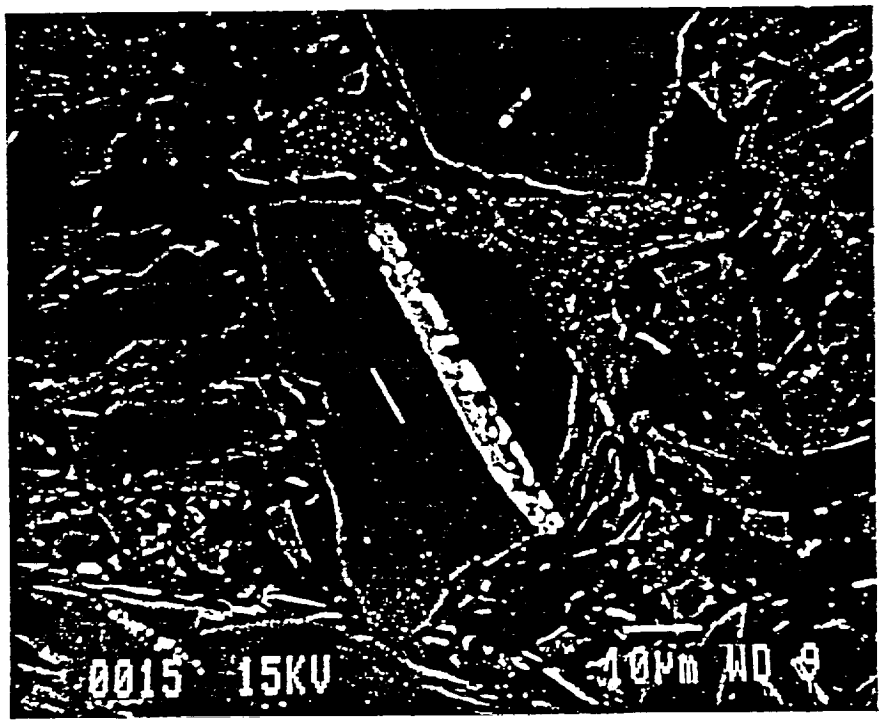

Figure 3.3 SEM Micrograph of a Cross Section of Partially Reduced Hypersthene

steady reaction rate. The reduction was much faster than either hypersthene or augite, with conversion approaching 90% after 3 hours. Additional experiments were made at 1270 K in 0.047 and 0.093 atm H_2 to determine the order of the reaction with respect to hydrogen. The order steadily increased from 0.57 at 20% conversion to 0.87 at 40% conversion (Figure 3.8). The apparent activation energy from the three experiments done at 0.14 atm H_2 is 204 kJ/mol (Figure 3.9). This did not change with conversion, and is the same as fayalite. Figures 3.10 and 3.11 are SEM micrographs of partially and completely reduced hedenbergite, respectively (Conversion calculated from mass loss data). In Figure 3.10, the dark grey phase is hedenbergite of the same composition as the starting material, light grey is Fa_{93}, and the white spots are iron. The Fa_{93} appears to be partially reduced, but the hedenbergite does not. Although a survey of the pellet showed that most of the grains are hedenbergite, a significant fraction are Fa_{93}. In Figure 3.11 (completely reduced hedenbergite), the white spots are iron. In the upper left is a grain that appears to be reduced ferrosilite. Some ferrosilite remains (grey phase) and the iron forms very large agglomerations in a silica matrix (very dark phase) in this area. The center grain is reduced Fa_{93}, with iron in a silica matrix. The other grains, more typical of the whole sample, are partially reduced hedenbergite. These consist of hedenbergite (light grey) with regions of a low iron product containing iron agglomerates. The composition of the low iron product is $Fe_{0.16}Mg_{0.06}Ca_{0.77}SiO_3$. This has the metal to silicon ratio of a pyroxene, but has too much Ca to lie in the region of stability for this family of minerals. The chemical formula is that of a pyroxenoid, which has a triclinic crystal structure. The powder pattern XRD of these two products is shown in Figure 3.12. The pattern of partially reduced hedenbergite shows α-iron, clinopyroxene, and some lines that could not be identified. These lines are not those of pyroxene, wollastonite (a pyroxenoid, $CaSiO_3$), olivine, or a crystalline form of silica. The pattern from the fully reduced hedenbergite shows α-iron, clinopyroxene, and cristobalite. This is the only evidence of crystalline silica found in any of the reaction products.

Discussion

The pyroxenes we used, because of their slow reduction rates and small mass losses, are difficult to study. The reduction curves (Figures 3.1, 3.4, and 3.7) of all three are similar, with an initial jump followed by a period of steady rate of reaction. Since the total mass loss for these minerals is small, desorption of water or other volatiles or preferential reduction of more reactive impurities could cause this. The amount of volatiles was estimated and their effect corrected for in the same way as for fayalite. As the micrographs of hedenbergite indicate, the preferential reduction of impurities may be the cause of the initial jump. XRD did not show the presence of Fa_{93}, which indicates that it constitutes less than approximately 5 wt% of the sample, but some was found with SEM/EDS.

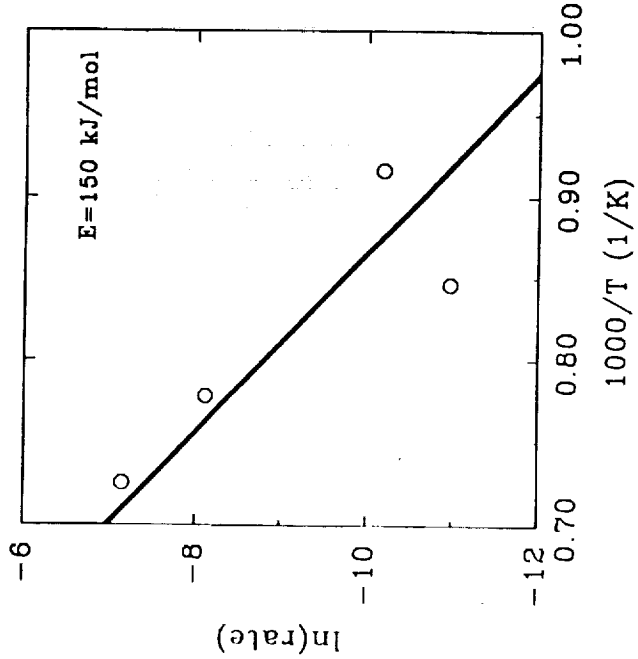

Figure 3.5 Apparent Activation Energy of the Reduction of Augite with H_2

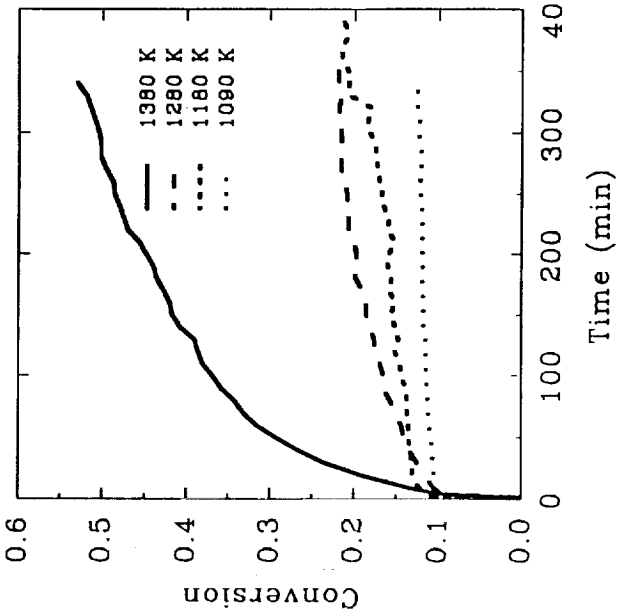

Figure 3.4 Reduction of Augite in 0.14 atm H_2

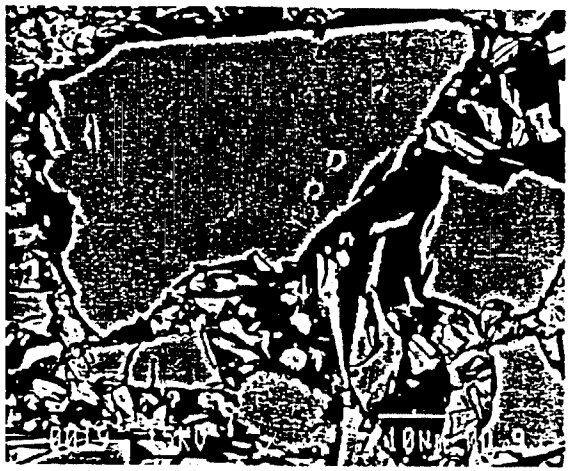

Figure 3.6 SEM Micrograph of a Cross Section of Partially Reduced Augite

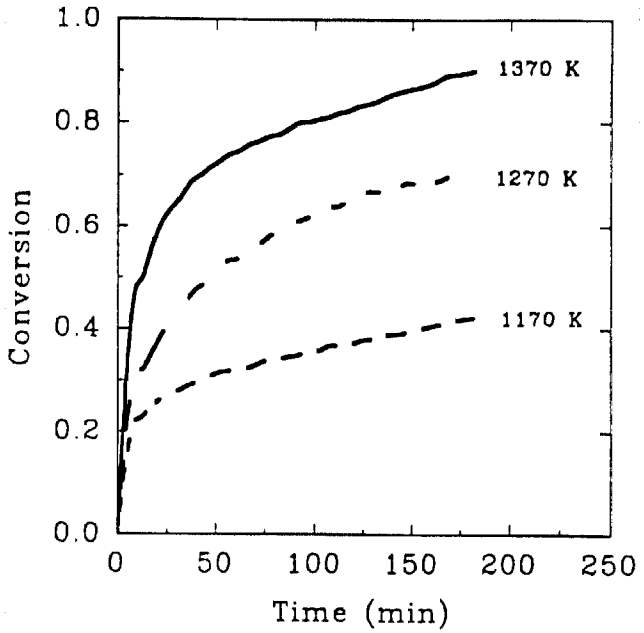

Figure 3.7 Reduction of Hedenbergite in 0.14 atm H_2

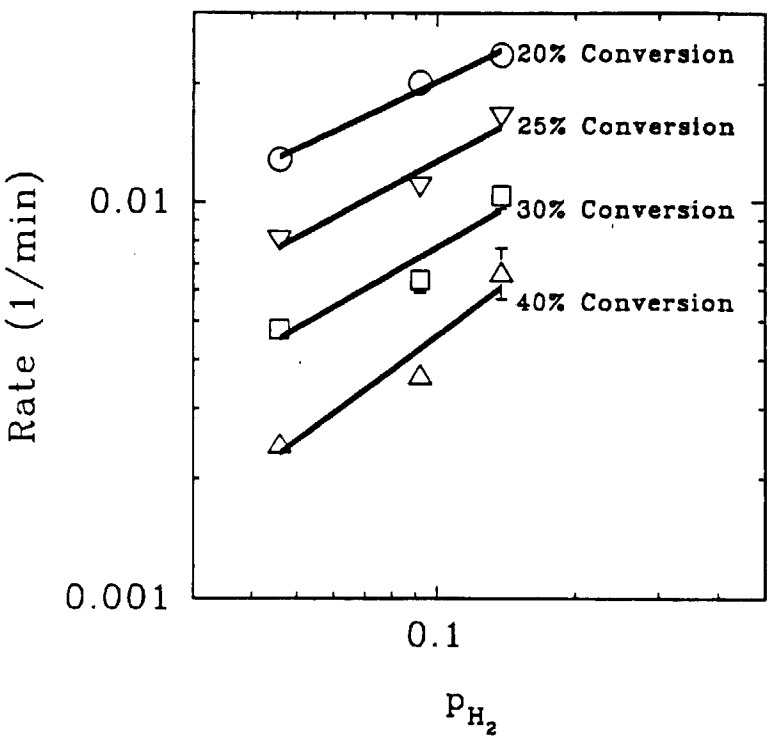

Figure 3.8 Effect of Hydrogen Partial Pressure on the Reduction of Hedenbergite

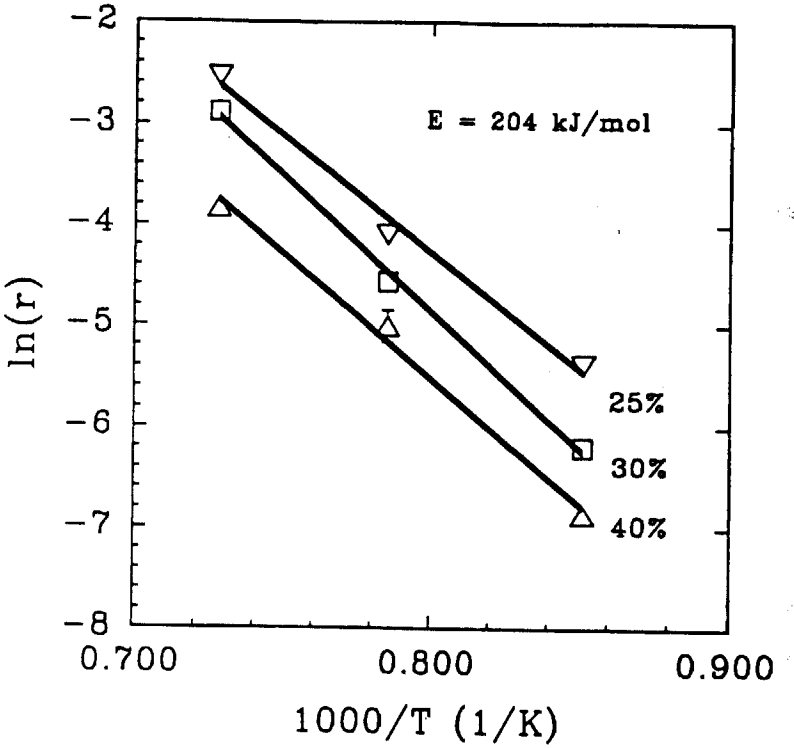

Figure 3.9 Apparent Activation Energy of the Reduction of Hedenbergite with H_2

Figure 3.11 SEM Micrograph of a Cross Section of Completely Reduced Hedenbergite

Figure 3.10 SEM Micrograph of a Cross Section of Partially Reduced Hedenbergite

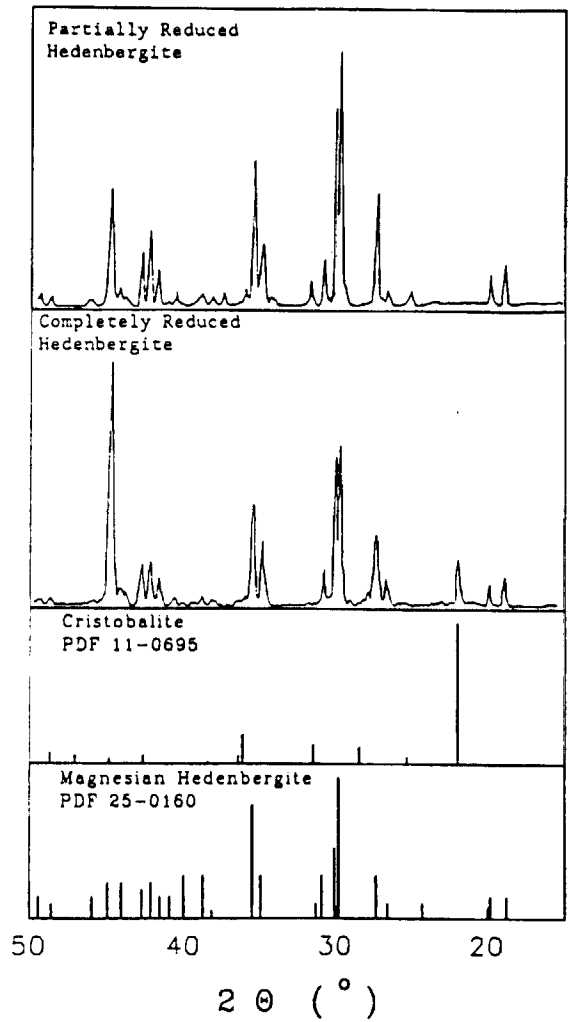

Figure 3.12 Powder Pattern X-ray Diffraction of Reduced Hedenbergite

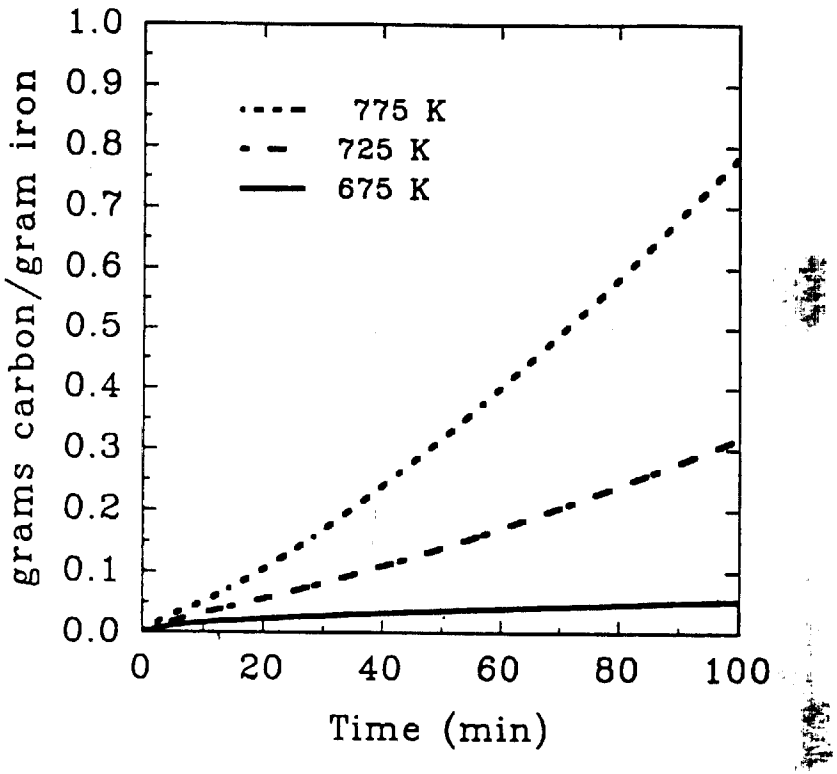

Figure 4.1 Deposition of Carbon on Iron in 0.08 atm H_2 and 0.26 atm CO

Ilmenite inclusions in the hypersthene (Figure 3.3) also reduce faster than the pyroxene. However, none of the starting materials had impurities of more than 5 wt%, as shown by XRD. Also, the reduction of fayalite and ilmenite would not be completed in the first few minutes of reaction. That all three, from different sources, had the same shaped reduction curve indicates that this may be a phenomenon intrinsic to the reaction of iron-bearing pyroxene with H_2.

The apparent activation energy varied considerably for the three minerals, generally increasing with Ca content, from 72 kJ/mol for hypersthene, to 150 kJ/mol for augite, and 204 kJ/mol for hedenbergite. The activation energy of hedenbergite did not change with conversion. The agreement between apparent activation energy of hedenbergite and Fa_{93}, the major impurity, seems suspicious. Further experiments with this mineral should be performed to determine if this is a reflection of the reduction of fayalite or a coincidence. The order of hydrogen pressure dependence in the reduction of hedenbergite increased steadily with conversion, from 0.57 at 20% conversion to 0.87 at 40% conversion. This suggests that the intrinsic order is 1/2, and the apparent order rises as diffusion through the growing product layer becomes more important in determining the rate. However, the micrographs of reduced hedenbergite show a product phase forming throughout the grain and not on the outside, so that the distance that H_2 must diffuse through the products is not increasing. This implies that diffusion through a layer of products is not important.

The product morphology in pyroxene reduction differs greatly from fayalite. For all three pyroxenes, the reduction appears to occur throughout the grain, and not along a reaction front separating products and an unreacted core. Hedenbergite was the only pyroxene with a silica product. Augite and hypersthene had very small specks of iron form, mainly but not exclusively on the outside of grains. Hedenbergite formed a product with a chemical formula similar to wollastonite, a pyroxenoid, but no pattern similar to wollastonite's appeared in XRD. It could be that the change in the Si-O lattice from clinopyroxene to wollastonite is too great to allow fast recrystallization, similar to the situation with fayalite. Cristobalite, the high temperature polymorph of SiO_2, was also formed. It formed at 1370 K, below the temperature of thermodynamic stability (1740 K). However, this mineral is known to form outside of its phase field if conditions are favorable, especially if crystallization is rapid (Berry and Mason, 1959). The iron in reduced ferrosilite forms large agglomerations, suggesting that it remains mobile. The iron formed in the reduction of hedenbergite also seems to be able to form large agglomerations.

The reduction of pyroxene is a complicated subject, and the study presented here gives only

preliminary findings. With only three different pyroxenes, the dependence of kinetic parameters on the chemical composition cannot be determined. The results do show some important difference from fayalite. The activation energy depends on the composition of pyroxene. The solid products do not form a layer around a shrinking core, but form throughout the grain. The order of hydrogen increases from 0.57 to 0.87 with conversion, suggesting a change of mechanism from one of 1/2 order to one of first order as the reaction proceeds. Further experiments are necessary to reach firm conclusions.

Carbothermal Reduction of Iron Bearing Minerals

Experiments

The general procedure used for carbon deposition and reduction experiments was the same as that for olivine. However, because the large changes in volume during the experiment would probably cause a pressed pellet to disintegrate, powdered samples were used instead. The powder was placed in a small quartz bucket (1 cm i.d., 1.5 cm deep) suspended on the microbalance. Iron titanate (CERAC, 99.9% pure) and iron (Alfa Catalog Chemicals) were used in experiments to find a suitable catalyst and conditions for carbon deposition. Both powders are -45 μm. The gas mixture used for these experiments was 0.08 atm H_2 and 0.26 atm CO in N_2. The outlet gas was monitored continuously with a nondispersive infrared analyzer for CO and CO_2. The amount of carbon deposited was measured by mass gain during the experiment, CO_2 in the outlet gas, and by monitoring mass changes while burning off deposited carbon in air after the deposition experiment.

Deposition/reduction experiments were performed with iron titanate (CERAC) and Fa_{93}. The iron titanate was the same as was used for the deposition experiments, and also for the reduction experiments of Yi Zhao (Zhao, 1991). A gas mixture of 0.23 atm CO and 0.02 atm H_2 was used for both prereduction and deposition. The ilmenite was reduced in this gas at 1270 K to 25% conversion, and the furnace was lowered to stop the reaction. After the furnace had cooled to the deposition temperature, it was raised and the deposition begun. When the desired amount of carbon had been deposited, the furnace was again lowered to stop the reaction. The CO and H_2 were turned off, and the system purged with N_2 for at least 2 hours. The furnace, heated to the reduction temperature, was raised to start the reduction reaction. The Fa_{93} used for deposition/reduction experiments was the same as that used for the H_2 reduction experiments. The only change in the experimental procedure for ilmenite was during prereduction. Since Gaballah *et al.* reported that CO did not reduce fayalite to any extent, 0.14 atm H_2 was used instead of the CO/H_2 mixture.

Results

The results to find a catalyst for carbon deposition are summarized in Table 4.1.

Table 4.1 Catalysts of CO Disproportionation

Catalyst	Conditions	Analysis	Result
$FeTiO_3$	643 K to 833 K up to 30% CO in N_2	TGA, Nondispersive Infrared analysis, Burn off C	Did not catalyze carbon deposition
Fe	643 K to 833 K up to 30% CO in N_2	TGA, Nondispersive Infrared analysis, Burn off C	Did not catalyze carbon deposition
Fe	673 K to 773 K 20% to 30% CO 2% to 9% H_2 in N_2	TGA, Nondispersive Infrared analysis	Catalyses carbon deposition

Ilmenite did not catalyze the CO disproportionation reaction. No weight gain or CO_2 in the outlet gas were observed. In some experiments with iron without H_2 in the gas stream, a small amount of CO_2 was observed in the outlet gas at the start of the experiment before the temperature stabilized and reliable weight measurements were possible, but it lasted only a few minutes and no weight gain was seen after the system temperature stabilized. The results of deposition experiments using iron and a gas mixture of 0.08 atm H_2 and 0.26 atm CO are shown in Figure 4.1. The deposition was slow and the rate steady at 680 K. At 730 K and 780 K, the rate was much higher and increased throughout the experiment.

Since iron in the presence of H_2 can catalyze carbon deposition, partially reduced ilmenite or fayalite should also do so, since there is some iron in the reduction products of these minerals. The gas mixture used for deposition of carbon on these minerals was 0.23 atm CO and 0.02 atm H_2. Figure 4.2 shows the deposition of carbon on 27% reduced $FeTiO_3$ and 27% reduced Fa_{93} at 750 K in this gas mixture. The deposition (per gram iron) was slower for both partially reduced minerals than for iron only, and the deposition on Fa_{93} was slower than $FeTiO_3$. However, both showed the steadily increasing rate observed with iron in this temperature range.

Reduction of ilmenite and Fa_{93} with deposited carbon at 1270 K is shown in Figures 4.3 and 4.4, respectively. Two experiments were performed with ilmenite, one with excess ilmenite and one with excess carbon. Reduction in both cases was very rapid until one of the reagents was consumed,

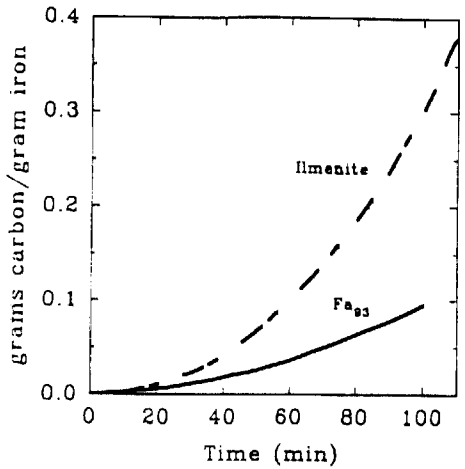

Figure 4.2 Deposition of Carbon on 27% Reduced Ilmenite and 27% Reduced Fe_{93}

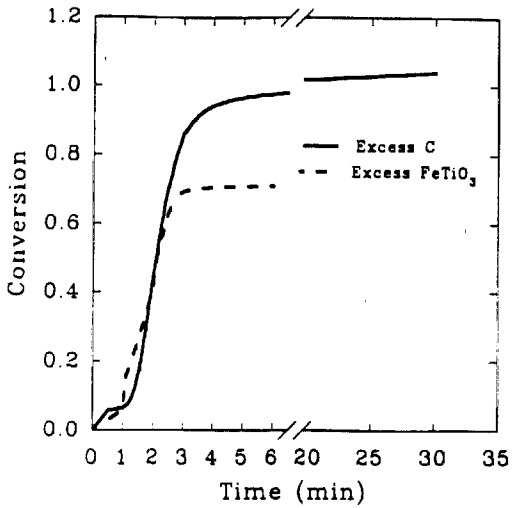

Figure 4.3 Reduction of Ilmenite with Deposited Carbon

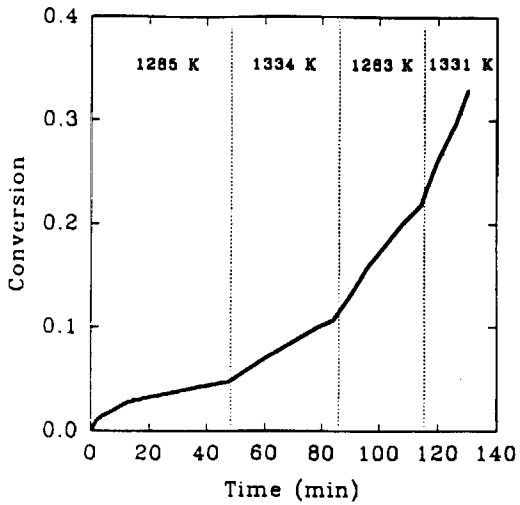

Figure 4.4 Reduction of Fe_{93} with Deposited Carbon

the reaction lasting only two or three minutes. When excess carbon was used, the weight loss continued, albeit much more slowly, until the experiment was stopped after 30 minutes. The conversion in this experiment reached values above 1, indicating that some TiO_2 may have reacted with the carbon. Reduction of Fa_{93} with deposited carbon was much slower. The temperature was raised in steps of about 50 K from 1280 K to 1430 K to observe its effect on reaction rate. Even at the higher temperature, reduction was not complete when the experiment was ended after 135 minutes. In all the carbothermal reduction experiments, only CO and no CO_2 was observed in the product gas.

Discussion

As one would expect from the literature, iron catalyzes CO disproportionation in the conditions of interest for the deposition reactor only when H_2 is present. Ilmenite did not catalyze the reaction under any conditions, and judging from the lack of extensive carbon deposits on the quartz glass reactor, silicates do not catalyze the reaction either. This is an advantage for the process, since it allows deposition of carbon only on the minerals and not on the reactor walls.

Deposition was slower on partially reduced ilmenite or partially reduced Fa_{93} than on iron powder. This is because the iron on partially reduced minerals is less accessible to the gas than iron powder, and so has less active surface area at the start of deposition. Deposition on Fa_{93} is slower than on ilmenite because the iron produced by reducing fayalite is mixed in a silica glass matrix and is sealed off from the CO. In both cases, the deposition rate steadily increases as carbon growth fragments the iron and surrounding materials, increasing the active surface area.

Deposited carbon rapidly reduces ilmenite, and achieved conversions above 1 after relatively short times. Final conversion above 1 indicates that TiO_2 formed in the initial reduction of ilmenite is reacting with carbon. The product of this reaction may be a substoichiometric titanium oxide (such as $TiO_{1.9}$) or titanium carbide (TiC). Although the higher O_2 production caused by this further reaction is beneficial for the production of lunar O_2, formation of TiC would present a problem. Since carbon is scarce on the Moon, nearly all the carbon used for reduction must be recovered and recycled. Recovering it from TiC may present difficult problems. A related problem is the possibility of forming Fe_3C, since iron may be in close contact with carbon during reduction. The nature of carbothermal reduction products is an area which needs further study. The reduction of fayalite with deposited carbon was much slower than ilmenite, but still took place at an appreciable rate. This is in contrast with the reduction of fayalite with CO, which Gaballah *et al.* report did not occur to

any extent. Gaballah *et al.* attribute the slow reaction between fayalite and CO to the formation of Fe_3C, which increased the volume of the reduction products and sealed the reaction front from further reaction. This should also occur during reduction with carbon, but apparently did not. If the reaction products are a mixture of iron in silica glass, as they are for reduction with H_2, it is not clear how the reducing agents can cross the product layer. Further study is needed to find the reaction mechanism.

The experiments done here indicate that a carbothermal reduction process for oxygen production on the Moon may be feasible. Because the use of a deep bucket to hold the minerals causes diffusion resistance, no kinetic parameters were derived. Much work remains to be done on this process. A reactor system that does not have diffusion resistance must be designed to derive the kinetics of the reactions. Carbon in the products (dissolved in iron, or as Fe_3C or TiC) is a real concern and must be investigated. However, the carbothermal reduction process works for ilmenite and fayalite, and is a promising alternative to gas reduction processes.

Conclusions and Recommendations

This study has determined the kinetic parameters and important steps of the reaction mechanism for the reduction of fayalite with hydrogen at partial pressures between 0.046 atm and 0.14 atm. The apparent activation energy is 212±5 kJ/mol and did not change much with magnesium content. The reaction is 0.8 order in hydrogen. The solid reaction products are silica glass and iron, with the iron intimately mixed in a silica matrix. Reaction kinetics are influenced by the permeation of H_2 through the silica and chemical reaction of dissociated H_2 with fayalite. An intermediate depleted in FeO is formed and iron is mobile in it, but on further reduction it forms glass, and the iron is immobilized.

The kinetics of reduction of pyroxene by H_2 is more complicated than fayalite due to the greater variations in chemistry of this mineral. The apparent activation energies for reduction in 0.14 atm H_2 are 72 kJ/mol for hypersthene, 150 kJ/mol for augite, and 204 kJ/mol for hedenbergite. Activation energy increased with calcium content. The hydrogen dependence of reduction of hedenbergite increases with conversion from 0.57 at 20% conversion to 0.87 at 40% conversion. Although this suggests that diffusion is increasingly important in the kinetics as the reaction proceeds, SEM micrographs show products mixed throughout the pyroxene and not forming a layer on the outside, which implies that the diffusion path length is not increasing. The iron appears to

remain mobile in the products, and cristobalite was formed in the reduction of hedenbergite at 1370 K.

The preliminary experiments reported here show that the carbothermal reduction of iron-bearing lunar minerals is possible. Carbon can be deposited from CO using the iron metal in partially reduced minerals as a catalyst if a small amount of H_2 is present. Reduction of ilmenite with deposited carbon is very rapid at 1270 K, and conversions above 1 are possible, indicating that the carbon is reacting with the TiO_2 formed in the reduction of ilmenite. Reduction of fayalite at 1270 K with carbon is much slower, but proceeds at a reasonable rate.

Recommendations

Much work remains to be done on the reduction of olivine with H_2. An oxygen production plant will use hydrogen pressures higher than those used here, so experiments should be done to see if the kinetic parameters derived at low pressures hold for higher pressure. Olivines higher in magnesium than the fayalites used here should be made and their reduction studied. Avoiding compositional zoning due to fractional crystallization will be very important in olivine synthesis. Other metal substituents may have a different effect than magnesium, so olivines containing them should be reduced. The Smithsonian Institute has donated some natural olivines to this project, some of which have significant amounts of manganese. Since Mn^{+2} is the most common metal in lunar olivine after Mg^{+2} and Fe^{+2}, these will provide good materials for reduction experiments. The loss of reactants is important in the design of a lunar oxygen plant, and significant amounts of H_2 and H_2O can be chemically bound in silica glass (Lee, 1962). The amount of hydrogen that remains in the silica should be determined.

Further work with pyroxene depends on successful synthesis of this mineral. A series of minerals with compositions varied so that a systematic study of the effects of composition on reduction kinetics should be made. Experiments to find the cause of the extremely rapid mass loss in the first few minutes of the experiments are needed. A thorough examination by SEM of the products of a reaction stopped just after this period is the first place to start. Synthesized minerals should also allow determination of whether impurities are responsible for the rapid mass loss during the first few minutes of the experiment. As with olivine, experiments should be performed to determine if the kinetic parameters derived here hold at higher hydrogen pressure.

The most important problem for carbothermal reduction of iron-bearing minerals is loss mechanisms

for carbon. The formation of carbides of iron, titanium, and silicon during reduction will make carbon recovery difficult. TiC and SiC should be easily identified with XRD, but the patterns for Fe_3C and Fe are very similar and other methods may be needed to differentiate between them. The kinetic parameters for deposition of carbon and reduction with carbon and their dependence on initial conversion, mineral composition, and other process variables should be determined. The carbothermal reduction of pyroxene can be investigated when a sufficient supply of pyroxene has been synthesized.

References

Audier, M.; Coulon, M.; Bonnetain, L. Disproportionation of CO on Iron-Cobalt Alloys I. Thermodynamic Study. *Carbon*, **1983**, *21*(2), 93-97.

Bell, T.; Hetherington, G.; Jack, K. H. *Phys. Chem. Glasses*, **1963**, *3*, 141.

Berliner, L.D.; Shapovalona, R.D. Thermodynamics of the Equilibrium of Fayalite (Iron Orthosilicate) with Hydrogen. *Russian Journal of Physical Chemistry* **1966** *40* (11), 1561-62.

Berry, L. G.; Mason, B. *Mineralogy Concepts Descriptions Determinations*, W. H. Freeman and Company, San Francisco, Ca. **1959**.

Birle, J. D.; Gibbs, G. V.; Moore, P. B.; Smith, J. V. Crystal Structures of Natural Olivines. *Amer. Min.* **1968,** *53*, 75-80.

Bliel, U.; Petersen, N. In *Landolt-Börnstein Numerical Data and Functional Relationships*: Springer-Verlag, New York **1982** N.S. V/1b, 317-20.

Bowen, N. L.; Shairer, J. F. The System, MgO-FeO-SiO_2. *Am. J. Sci.*,5th ser. **1935**, *29*, 174-80.

Briggs, R. A.; Sacco, A. Hydrogen Reduction Mechanisms of Ilmenite Between 823 and 1353 K. *J. Mater. Res.* **1991**, *6* (3), 574-84.

Chase, M. W., Jr.; Davies, C. A.; Downey, J. R., Jr.; Frurip, D. J.; McDonald, R. A.; Syverud, A. N. JANAF Thermochemical Tables. *J. Phys. Chem. Ref. Data* **1985** Suppl.

Cutler, A. Power Demands for Space Resource Utilization. *Space Nucl. Power Syst.*, **1986**, 25-42.

Cutler, A. H.; Waldron, R. D. Evaluation of Processing Options for Lunar Oxygen Production. Proceedings of Space '92, ASCE, Denver, CO, June 1-4, **1992**.

Deer, W. A.; Howie, R. A.; Zussman, J. *Rock Forming Minerals*, 2nd ed.; Halsted Press: N.Y., 1982.

Gaballah, I.; Jeannot, F.; Gleitzer, C.; Dufour, L. C. Cinétique de Réduction de l'Orthosilicate de Fer Fe_2SiO_4 (Fayalite) par H_2, CO et les Mélanges $CO+H_2$. *Mém. Sci. Rev. Métallurg.* **1975**.

Guinot J.; Audier, M.; Coulon, M.; Bonnetain, L. Formation and Characterization of Catalytic Carbons Obtained from CO Disproportionation Over an Iron Nickel Catalyst. *Carbon* **1981** *19* 95-98.

Heiken, G. H.; Vaniman, D. T.; French, D. E., *eds. Lunar Sourcebook*: Cambridge Univ. Press, 1991.

Lee, R. W. Diffusion of Hydrogen in Fused Quartz. *J. Chem. Phys.* **1963**, *38* (2), 448-55.

Lee, R. W.; Frank, R. C.; Swets, D. E. Diffusion of Hydrogen and Deuterium in Fused Quartz. *J. Chem. Phys.* **1962**, *38* (4), 1062-71.

Minowa, S.; Yamada, M.; Torii, C. *Tetsu to Hagane* **1968** *54* (12) 1203-16.

Olsson, R. G.; Turkdogan, E. T. Catalytic Effect of Iron on Decomposition of Carbon Monoxide:II. Effect of Additions of H_2, H_2O, CO_2, SO_2, amd H_2S. *Met. Trans.*, **1974**, *5*, 21-26.

Shackelford, J. F.; Masaryk, J. S. The Thermodynamics of Water and Hydrogen Solubility in Fused Silica. *J. Non-Crystalline Solids*, **1975**, *21*, 55-64.

Shomate, C. H.; Naylor, B. F.; Boericke,F. S. Thermodynamic Properties of Ilmenite and Selective Reduction of Iron in Ilmenite. *U.S. Bureau of Mines Report of Investigations 3864*, **1946**.

Turkdogan, E. T.; Vinters, J. V. Catalytic Effect of Iron on Decomposition of Carbon Monoxide: I. Carbon Deposition in H_2-CO Mixtures. *Met. Trans.*, **1974**, *5*, 11-19.

Wagman, D. D.; Kilpatrick, J. E.; Taylor, W. J.; Pitzer, K. S.; Rossini, F. D. Heats, Free Energies, and Equilibrium Constants of Some Reactions Involving O_2, H_2, H_2O, C, CO, CO_2, and CH_4. *J. Res. NBS*, **1945**, *34* 143-61.

Waldron, R. D.; Cutler, A. H. Evaluation of Processing Options for Lunar Oxygen Production. Proceedings of Space '92, ASCE, Denver, CO, June 1-4, **1992**.

Walker, P. L.; Rakszawski, J. F.; Imperial, G. R. Carbon Formation From Carbon Monoxide Over Iron Catalysts. II. Rates of Carbon Formation. *J. Phys. Chem.*, **1959**, *63*, 140-49.

Watanabe, K.; Tanimura, T.; Yoshii, Y. Study of Reduction in Systems of Wüstite, Silica, and a Third Oxide. *Hokkaido Daigaku Kogakuku Kenkyu Hokoku* **1968** *48* 45-54.

Yanagihara, T.; Kobayashi, T. The Reduction of Fayalite with Hydrogen. *Nippon Kinzoku Gakkai shi* **1969**, *33* (3), 313-17.

Zhao, Y. Doctoral Diss., Dept. of Chemical Engineering, University of Arizona, Tucson, AZ., **1991**.

Zhao, Y.; Shadman, F. Reduction of Ilmenite with Hydrogen. *Ind. Eng. Chem. Res.* **1991**, *30*, 2080-2087.

Zhao, Y.; Shadman, F. Kinetics and Mechanism of Ilmenite Reduction with Carbon Monoxide. *AIChE J.*, **1990**, *36*(9), 1433-38.